SEDIMENT TRAP RECORDS OF DEPOSITION IN LALLEMAND FJORD ADJACENT TO MÜLLER ICE SHELF, ANTARCTIC PENINSULA.

by

ÅSA CHONG

A thesis submitted to the Department of Geography

in conformity with the requirements for

the degree of Master of Science

Queen's University

Kingston, Ontario, Canada

July, 2000

Abstract

The Müller Ice Shelf is situated in Lallemand Fjord on the western side of the Antarctic Peninsula. It has an area of about 80 km^2 but is currently retreating and has reached its minimum recorded extent. The disintegration of this ice shelf and other ice shelves in the area has been attributed to the 2.5°C warming trend recorded in the area over the past 50 years. This research seeks to understand the sedimentary record in proximity to the Müller Ice Shelf. Such records relate to the historical fluctuations of ice shelves in general, and the significance of the present changes in relation to natural variations.

As part of the sedimentological studies in Lallemand Fjord, sediment traps were deployed for more than a year in front of the Müller Ice Shelf. The purpose of the study was to determine: 1) the origin of the sediment, 2) how the sediment sources change with climate, 3) how sediment is distributed throughout the fjord, 4) the relationship between trapped sediment and the depositional processes as inferred from sediment cores.

Sediment in traps consisted mostly of dark gray to black clay and silt. Sand was present in all traps with small peaks in top and/or bottom of proximal sites that could reflect seasonal deposition. Biogenic content was low compared to sediment from fjords to the north but also showed peaks that could indicate seasonal productivity. Ice rafting occurred throughout the period of deployment. The measured annual flux in all traps except the mid-water distal trap agrees with the sedimentation rate of 1-2 mm a^{-1} calculated from sediment cores.

Sediment deposited at the Müller Ice Shelf comes from aeolian debris, basal melt of the ice shelf, ice rafted debris, and biogenic products. Some of this sediment is transported away from the source by mid-water currents. Colder conditions at this site would reduce the amount of biogenic production in the water column during spring, as it is dependent on ice melt. It would also reduce the amount of ice rafted debris because less calving would occur. More aeolian debris might be transported due to increased wind activity in colder conditions. However, the flux of aeolian debris to the water column could decrease due to permanent sea ice or decreased calving.

Co-authorship

- Geochemical analysis of sediment was done at Stanford University by Dr. R. Dunbar.
- Dr. R. Gilbert performed the subbottom acoustic survey in front of the Müller Ice Shelf in 1998.
- Diatom identification was done at Colgate College by Dr. A. Leventer.
- All other aspects of analysis were done by the author.

Acknowledgments

I would like to thank my supervisor Dr. R. Gilbert for giving me the opportunity to do this project and for advice on the thesis and help with preparing the moorings prior to deployment. I also thank co-chief scientists Dr. E.W. Domack and Dr. A. Leventer for their support during this thesis.

Funding was provided by a grant from the Natural Sciences and Engineering Research Council of Canada (NSERC) to Dr. Gilbert and a grant from the National Science Foundation (NSF) to Dr. Domack and Dr. Leventer.

The endless help with thin section preparation by Dr. S. Lamoureux as well as the use of his lab is greatly appreciated.

Thanks to Dr. R. Dunbar for the use of the sediment trap mold, for the geochemistry analysis, and to him and D. Mucciarone for help with trap retrieval.

The crews on *Lawrence M. Gould* and *Nathaniel B. Palmer* are thanked for their work during sediment trap deployment and retrieval.

Thanks go out to the members of D108 for making our office a friendly and fun place to work, especially to Erin for fruitful discussions. Thanks also to the pottery gang for fun Thursday evenings, and Brandon and Paul for computer help.

I thank my parents, siblings, and Mary and Jack for their support and encouragement during my studies.

Finally, I thank my husband Steve for his endless support and encouragement.

Table of contents

List of Tables

List of Figures

Chapter 1: Introduction

1.1 Introduction

The Antarctic Peninsula (AP) has experienced an air temperature increase over the past 50 years. Vaughan and Doake (1996) noted that this temperature increase caused a southward shift of the mean annual isotherms across the peninsula. During this time there was a corresponding rapid retreat and disintegration of large ice-shelves (Nicholls, 1997; Vaughan and Doake, 1996; Skvarca, 1993; Doake and Vaughan, 1991), recorded decline in sea-ice extent (de la Mare, 1997), observed increase in the duration of the summer melt season (Ridley, 1993), and observed changes in penguin nesting sites (Emsile *et al.*, 1998) in the region. It is not known how much of this change has been caused by anthropogenic impact on the environment and how significant this change is in relation to natural climate variability. Therefore, an understanding of the historical climate is needed.

To study the climate history of this region it is necessary to go beyond the relatively short instrumental records and use proxies, such as sediment, as clues to past conditions. Variability in sediment composition and sedimentation rate can be used to infer the environmental context of deposition (Smith *et al.*, 1999). Such inferences can be made if there is a knowledge of modern sedimentary processes. For this purpose, sedimentological studies on depositional processes and water column productivity (e.g. Domack and McClennen, 1996; Leventer *et al.*, 1996; Leventer and Stevens, 1996; Domack *et al.*, 1995; Domack and Ishman, 1993; Mammone, 1992) have been carried out along the

west side of the AP. Because of the apparent sensitivity of ice-shelves to temperature change, some studies have concentrated specifically on understanding the signals in sediment associated with these environments (e.g. Domack *et al.*, 1995; Stein, 1992). One site for such studies has been the Müller Ice Shelf (MIS), Lallemand Fjord, the most northern ice shelf on the west side of the AP and the site of this thesis project.

1.2 Study site

Lallemand Fjord is situated on the western side of the AP at 67°S, 66°W near Adelaide Island (Fig. 1.1). The peninsula is a mountainous region, reaching elevations of 2000 m along most of its length. This ridge acts as a barrier to cold continental air moving west from the Weddell Sea and creates a divide between relatively mild maritime conditions in the west and cold continental conditions in the east (King and Turner, 1997). Milder conditions are produced by cyclonic storms originating in the Amundsen Sea, which move eastward, and which are deflected north along the high ridge of the Peninsula (Griffith and Anderson, 1989).

In the north-south direction there are strong temperature gradients. The mean annual temperatures range from -3 to - 17°C (Reynolds, 1981) and as a result, there are three distinct glacial maritime regions in the area: polar, sub-polar, and temperate (Domack and McClennen, 1996; Griffith and Anderson, 1989). The MIS is situated at the -5°C mean annual isotherm (Reynolds, 1981),

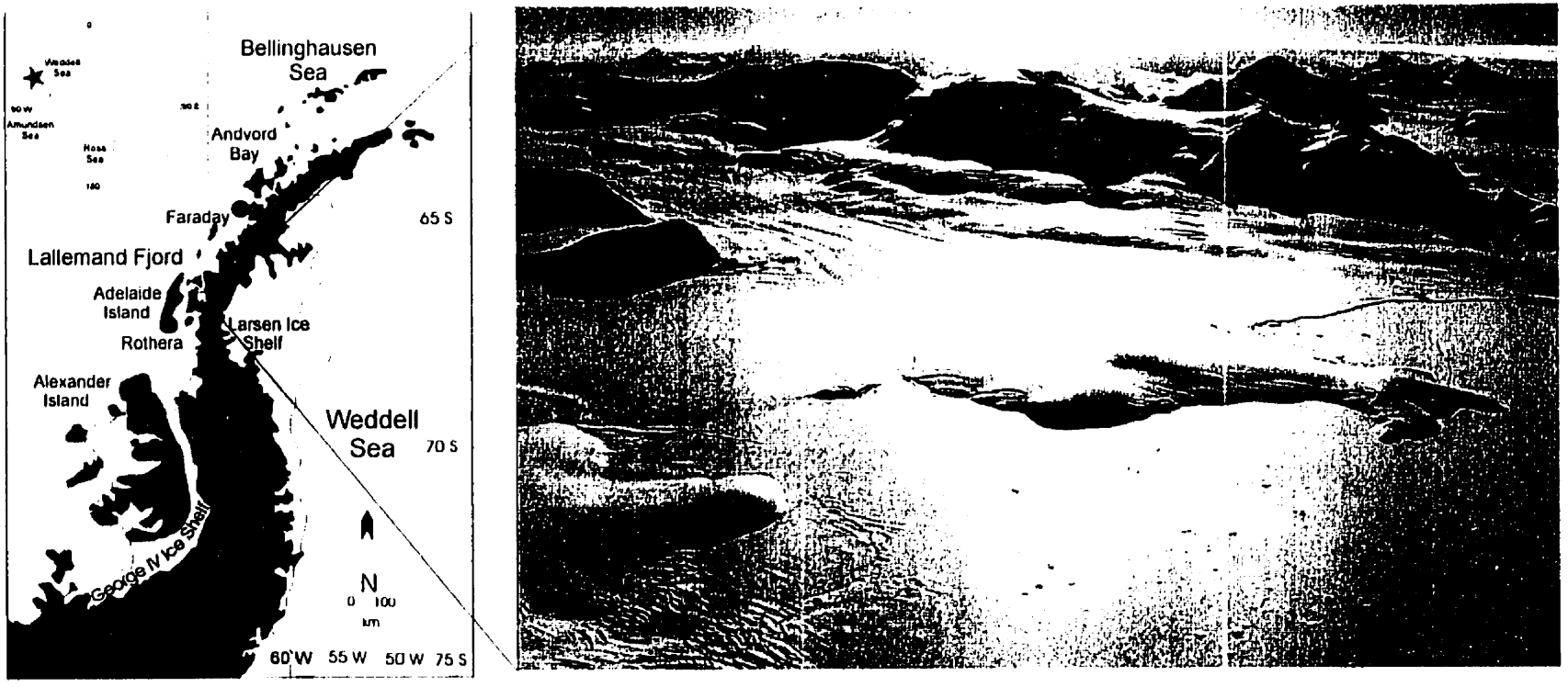

Fig. 1.1 Map showing the study location in Lallemand Fjord and the British research station Rothera from which meteorological data were obtained. Oblique view looking SSW over the Müller Ice Shelf in November 1996. Photo courtesy D. Vaughan, British Antarctic Survey.

which is the limit of ice shelf viability (Vaughan and Doake, 1996). There are no measured meteorological data from Lallemand Fjord. The nearest research station is at Rothera on Adelaide Island. Monthly mean temperatures measured between 1976 and 2000 show inter-annual temperature variations that are especially large in winter (Fig. 1.2). The same pattern has been seen in temperature measurements further north at Faraday station (65.3° S, 64.3° W: King and Turner, 1997) and because the temperature anomalies are associated with long lag periods, it suggests that temperatures in the region are influenced by ocean circulation and temperature (King and Turner, 1997). There is also an observed correlation between sea ice extent and temperature in the Bellinghausen Sea which may suggest that the peninsula region is affected by small changes in the ice edge position (King and Turner, 1997).

The bathymetry of Lallemand Fjord reveals a series of basins generally oriented in a north-south direction (cruise report, NBP9903). There are two deep areas, one near the mouth of the fjord and one near the middle. These deeps are very steep-sided and reach depths between 1240 and 1500 m. The area near the ice shelf is shallower, the greatest depth being 700 m. A 550-m deep sill is found at the mouth of the fjord (Domack *et al.*, 1995).

Paleoenvironmental investigations of Lallemand Fjord reveal a dynamic setting. The fjord was deglaciated prior to 8000 BP (Shevenell *et al.*, 1996). A period of open marine conditions followed (8000 to 2700 BP) when the extent of

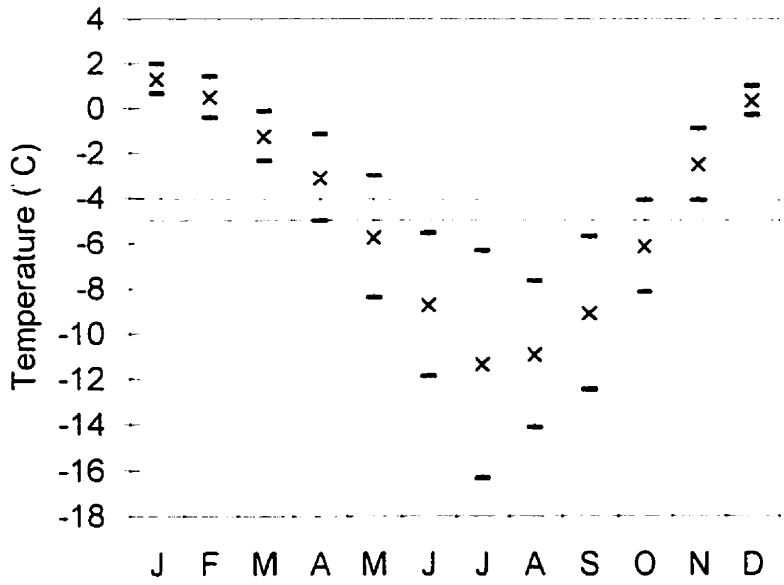

Fig. 1.2
Monthly mean temperatures at Rothera station between 1976-2000. Error bars show the interannual standard deviation. The dashed line indicates the mean annual isotherm below which ice shelves can be found and the solid line indicates mean annual temperature between 1976-2000 (-4.7 C)
Data supplied by the British Antarctic Survey, Cambridge. UK.

sea ice cover varied. A climatic optimum took place between 4200 and 2700 BP but around 2700 BP sea ice became more extensive and seasonally persistent.

The MIS formed in the Little Ice Age (LIA; Domack *et al.*, 1995). It is a small ice shelf (~80 km^2) fed by the Brückner and Antevs valley glaciers (Domack and McClennen, 1996; Ward, 1995). According to sediment studies and images of the ice shelf, it has been recorded that the MIS is retreating (Ward, 1995; Stein, 1992) and is at its minimum extent (Vaughan and Doake, 1996). Its continued presence has been attributed to the protective setting in the fjord and the fact that the ice shelf is pinned to the Humphrey ice rise (Shevenell *et al.*, 1996; Ward, 1995). At least three other tidewater glaciers enter the fjord, which means that icebergs are fairly abundant. The total ice drainage area of all glaciers is about 1290 km^2 (Domack and McClennen, 1996).

1.3 Background: results from previous studies

Since the MIS is currently receding (Ward, 1995; Stein, 1992), it has been possible to collect cores for sedimentological investigations in places that previously were covered by the ice shelf. Therefore, the down-core sedimentary record represents both ice-proximal as well as ice-distal environments. Cores were also taken with increasing distance from the present ice edge. A notable observation in the sediment was the abrupt decrease in sand content with distance from the ice shelf and the corresponding increase in total organic carbon (TOC). In addition, the proximal sand was very well-sorted compared to the sand collected at more distal sites. It was suggested that very well-sorted sand was associated with the ice shelf edge, whereas poorly sorted material was

found in more distal sites in connection with iceberg rafting (Domack *et al.*, 1995). These changes were also observed down-core in the cores from the previously ice covered area (Domack *et al.*, 1995; Domack and Stein, 1993). A theory was developed that if well-sorted sandy facies in the core were representative of an ice-proximal environment, a fluctuation of such layers in the core record could reflect fluctuations of the ice shelf edge.

As a result of these studies, a picture of the depositional setting in Lallemand Fjord has developed. It is believed that the well-sorted sand facies found today near the calving line of the MIS is of aeolian origin and was either deposited into the water column at the edge of the ice shelf, thus representing its frontal position, or fell through cracks in the ice upstream of the front, or from icebergs rafting seaward from the calving line. Silt and clay are slowly melted out from beneath the ice shelf, and dropstones are deposited in a more distal setting from icebergs, some of which originated elsewhere.

1.4 Objectives

To continue the sedimentological studies in this area, this project studied the sediment collected from the water column in front of the MIS during one year of deposition. Analysis of this sediment is compared with results from previous investigations and related to the theory on deposition put forth in these studies. The following questions were asked.

- What is the origin of sediment entering the fjord?
- How do sources change as environmental (principally climatic) factors change?
- How is sediment distributed through the fjord?

- How do deposits represent the sources (and their controls) and the distribution processes?
- What is the relationship between sediment recovered from the water column and the processes of deposition on the sea floor as indicated by cores?

Chapter 2 of this thesis contains a literature review focusing on glacimarine sedimentation with some focus on Lallemand Fjord. Chapter 3 discusses the field and laboratory methods used. Chapter 4 is a manuscript discussing the findings and conclusions of the study. Finally, Chapter 5 is a summary in which implications and possible future work are discussed.

Chapter 2: Literature review-Glacimarine sedimentation

2.1 Introduction

The definition of a glacimarine environment has been changed many times over the past 150 years. Changes in the definition reflect the evolution in knowledge and understanding of these complex environments (Anderson and Molnia, 1989). One modern definition used by Powell and Domack (1995, p. 445) is "a marine environment in sufficient proximity to glacial ice that a glacial signature can be detected within the sediment". The complexity of a glacimarine environment is attributed to the combined influence of sea and glacier ice, fresh and sea water, wind, and biologic activity on sedimentary processes and deposits.

Glacimarine environments in the Antarctic Peninsula range over climate zones including temperate, sub-polar and polar regions. It has been difficult to develop glacimarine sedimentary facies models based on climate zones because the depositional systems vary considerably even within the same zones (Anderson and Ashley, 1991; Anderson and Molnia, 1989). Of more importance to the sedimentary environment seems to be the oceanographic and physiographic regime of the area. Climate is secondary to these controls but has, together with the ice drainage basin size, an influence on the amount of sediment supplied to the setting (Domack and Ishman, 1993). In addition, the many different sediment sources and sediment distribution and redistribution

processes that act on the sediment add even more complexity to these environments.

This review is divided into sections of type of glacier termini, sediment sources, oceanographic influences on sedimentation, sediment distribution, and sediment redistribution.

2.2 Glacier termini - tidewater glaciers and ice shelves

Marine-ending glaciers cover most of the Antarctic coastline. Only 5% of the coastline is rock and sediment, 57% is occupied by floating glacier termini, and 38% grounded termini (Drewry *et al.*, 1982 in Powell and Domack, 1995). The type of glacier terminus determines how sediment is delivered to the water column, how temperature, salinity, and currents affect sedimentation, and what sedimentological processes take place in the proximal and distal environment (Powell and Domack, 1995; Drewry, 1986).

Tidewater termini are present in all Antarctic climate settings. They form vertical cliffs at sea level because the glacier calves faster than it melts (Powell and Domack, 1995). Calving can occur by fracturing above sea level and collapse of the ice face, or by shear back from the glacial face releasing large bergs, or by fracturing at depth releasing bergs to rise to the sea surface (Powell and Domack, 1995).

A floating terminus forms where glacier flow is unconstrained by the basal shear stress affecting a grounded glacier and is able to extend farther seaward and at a lower gradient. Extension is favoured where the glacier flows into an

embayment where it will be protected from the effects of tides and currents that tend to break up the ice tongue. In addition, localised high spots become pinning points for the shelf to stabilise around (Blankenship *et al.*, 1989). Ice mass increases through snow accumulation on the upper surface, from continuous flow of inland glaciers (Hulbe, 1997) and in some cases even by freezing of sea water onto the underside of the shelf (Hulbe, 1997; Nicholls, 1997).

2.3 Sediment sources

Glacier ice, icebergs, meltwater streams, and sea ice are the major sources of sediment in the glacimarine system. The volume and distribution of sediment within glacier ice is controlled by ice-dynamics and thermal dynamics (Drewry, 1986). For example, all basal ice in a temperate glacier is at the pressure melting point and the ice can incorporate a thin zone of basal debris by refreezing of meltwater in the lee of bedrock undulations. A thicker zone of basal debris can be incorporated in a sub-polar glacier when the upstream ice is at the pressure melting point, while downstream basal ice temperature is below that temperature. If all ice in a glacier is below the pressure melting point very little basal debris can be incorporated since the freezing on of debris cannot occur (Dowdeswell, 1987; Drewry, 1986). Debris can also be entrained passively on the surface of the ice as a result of rockfalls, debris avalanches, or aeolian deposition. If passive deposition takes place in the accumulation zone of the

glacier or if two glaciers converge, the debris can become englacial downstream.

2.3.1 Glacier ice

Debris that has been incorporated by glaciers is later released through melting. Melting of glacier ice in the ocean depends on the flux of heat into the ice from the surrounding sea-water and is also caused by changes in pressure, and thus the freezing point, of water flowing towards the grounding line (Drewry, 1986). Doak (1976, in Drewry, 1986) presented a formula describing the factors involved in ice melting:

$$M=(Q_s^{\cdot} - Q_i^{\cdot}) / \rho_i L$$

where M is the melt rate, $Q_s^{\cdot}$ is the heat flux from the sea, $Q_i^{\cdot}$ is the heat flux upward through the ice, ρ_i is the density of the ice, and L is the latent heat of fusion. One of the factors affecting $Q_s^{\cdot}$ is water temperature.

Basal ice shelf sediment can be released by melting (Drewry, 1986) within a few kilometres of the grounding line (Drewry and Cooper, 1981; Jacobs *et al.*, 1979). This becomes important in regions of Antarctica where the warm Circumpolar Deep Water (CDW) penetrates beneath ice shelves (Domack and Ashley, in preparation; Jenkins *et al.*, 1997). It has been suggested that the base of the Müller Ice Shelf is affected by CDW water that upwells in front of the shelf. Measures of temperature and turbidity indicate elevated temperature and higher turbidity possibly indicating basal melting and release of englacial sediment (Domack and Ashley, in preparation).

2.3.2. Iceberg rafted debris (IRD)

Icebergs are important features for debris transport and release. Their size, shape, and rate of formation is controlled by the morphology and dynamics of the parent ice mass (Dowdeswell and Dowdeswell, 1989). Sedimentation rates from icebergs are highest in Southeast Alaska, an order of magnitude lower in Svalbard, and four orders of magnitude lower in the High Arctic and the Antarctic Peninsula region. Even though the Antarctic icebergs commonly are much larger than the Alaskan, they are also most commonly barren (Syvitski *et al.*, 1996; Powell and Domack, 1995; Anderson *et al.*, 1980). However, the relative importance of IRD input may be larger in high polar settings where input from meltwater streams is smaller (Dowdeswell and Murray, 1990). In addition, Smith and Ashley (1996) emphasise the importance of initial berg size to the distribution of IRD, since the size of the iceberg is one factor that determines how fast it melts and thus how far it will move away from its source and deposit debris.

2.3.3. Meltwater streams

In temperate glacial settings, meltwater enters the ocean directly from marine glacial termini, or from streams creating sandurs between land-based glaciers and the sea. Discharge varies seasonally and diurnally, and relates to regional climate and glacier thermal regime (Dowdeswell, 1987). Most of the sediment is transported as particulate matter, either as suspended load or as bedload (Church, 1972). Although some sediment enters fjords from streams in

the northern Antarctic Peninsula, there is no fluvial discharge to the sea in the remainder of Antarctica (Anderson and Molnia, 1989).

2.3.4. Sea Ice

Sediment can be incorporated in sea ice during ice formation or accumulate on the sea ice surface as a result of wind action, stream discharge, rockfall, and wave and current wash-over (Syvitski and Shaw, 1995; Gilbert, 1983). During ice formation, fine-grained suspended sediment is used as nuclei for ice crystal growth in frazil ice. Sediment is scavenged from the water column by the rising frazil and commonly gives the resulting ice a darker colour. Sediment is also incorporated in sea ice during development of anchor ice. Cool, dense sea water sinks to the sea floor, nucleates around inorganic and organic material, and freezes. Eventually the ice becomes buoyant enough to rise, lifting the material that has been frozen into the ice (Gilbert, 1990; Drewry, 1986).

Sea ice is also important for the production of biogenic material that might later be incorporated in the sea floor sediment. Ice melt in the marginal ice zone results in stability of the water column. Productivity is enhanced by strong vertical stratification and also by the exposure of nutrient-rich water to increased sunlight. Blooms under such conditions are quantitatively significant in much of the Antarctic (Smith and Saukshaug, 1990). Sometimes blooms take place within the basal layers of sea ice and are later released upon melting (Dunbar *et al.*, 1998).

2.3.5. Aeolian processes

Aeolian processes in polar regions can be significant due to the cold air and high wind velocities in these regions. Cold air is more dense than warm air and the drag force on a particle moving in air increases with increasing air density. In addition, moisture losses through sublimation of frozen particles increase the amount of loose sediment during the colder season. The impact of snow particles on sediment under windy conditions, initiates sediment transportation. This form of sediment transport is important in polar regions since meltwater transport there is rare. In addition, sea ice acts as a suitable platform for saltation to take place (McKenna Neuman, 1993). For example, in a study of modern sedimentation Barrett *et al.*(1983) found wind-blown sand on sea ice both near the coastline, and about 35 km to sea from the coast in McMurdo Sound, Antarctica.

2.3.6. Biological production

Almost all organic carbon in Antarctic sediment is of autochthonous marine origin. Limited siliclastic sedimentation in polar climates decreases the amount of dilution of organic matter. In addition, high productivity at ice margins increases the amount of organic matter falling to the bottom and once there, the cold bottom water restricts bacterial metabolism at the sediment-water interface. Conversely, subpolar and temperate environments receive more meltwater input and thus more siliclastic material. Productivity is limited due to the reduced amount of sea ice, and warmer water creates higher rates of bacterial

metabolism (Powell and Domack, 1995). However, facies patterns cannot be related to these climate regimes solely based on these observations. Bathymetry, and oceanographic regimes (including the depth and velocity at which inflow is distributed in the sea water, Coriolis effect, interflows, and wind effects) also control the sediment signature. Nonetheless, it has been found that the ratio of texture and composition in relation to distance from an ice shelf can be used as a temporal indicator of glacial and sea ice fluctuations (Domack and Ishman, 1993; Stein, 1992).

2.4. Oceanographic processes and sedimentation

2.4.1. Overflow-estuarine circulation

Meltwater discharging from tidewater termini is greatest during the summer but can take place over longer periods of the year if basal melting occurs. When fresh water enters the denser sea water it tends to upwell higher in the water column since it is very buoyant (Powell and Domack, 1995; Dowdeswell, 1987; Drewry, 1986). At that point, which is almost always at the surface, it forms an overflow. As the freshwater sediment plume moves seaward from its source, a compensating flow of deeper, more saline water flows landward. During this process, mixing of the two water masses takes place by the mechanism of entrainment and diffusion (Drewry, 1986). Turbulent diffusion takes place if turbulent flow is present in both density strata. But the density gradient between saline and fresh water tends to inhibit momentum exchange by turbulent flow and therefore mixing is induced only if a critical shear occurs

between the two layers. The amount of entrainment occurs in response to the balance between density stabilising forces and the destabilising velocity shear (Drewry, 1986) and can be described by the Richardson number:

$$R_i = (g/\rho_w)(d\rho_w/dz)/(dU_w/dz)^2$$

where g is the acceleration due to gravity, ρ_w is the water density, $(d\rho_w/dz)$ is the density gradient, and (dU_w/d_z) is the velocity gradient, each with respect to depth over the potential mixing surface.

Estuarine circulation is not evident in Lallemand Fjord. The CDW enters the fjord and upwells at the ice shelf. However, there is no distinct decrease in salinity, as would be expected if fresh meltwater is introduced, and therefore it is difficult to discern how much the ice shelf is melting. Colder and fresher water is seen in the main axis of the fjord and is probably originating from outside (Domack and Ashley, in prep.).

2.4.2. Interflows

Interflows, called cold tongues, at mid-water depth, have been found in fjords of Antarctica (Domack *et al.*, 1994; Domack, 1990; Domack and Williams, 1990). Ice-proximal measures of salinity, temperature, and light transmissivity show a characteristic pattern with depth. Relatively cold and turbid water is inter-layered with the warmer and clearer surrounding water. Fractured silt-sized quartz grains collected from these cold tongues indicate that the sediment originated from the basal region of the glacier. Originally, Domack and Williams (1990) suggested that the cold tongues were derived by tidal pumping of basal

cavities. A later study by Domack *et al.* (1994) suggested that short time variation in basal meltwater discharge could be the cause of these features.

The mid-water cold tongues are important mechanisms for sediment transport below the surface and possibly also essential for sedimentary structures in the benthic deposits. For example, Domack (1990) found that interflows along the Danco Coast in the Antarctic Peninsula created thin-bedded laminated sedimentary structures.

Mid-water transport has been seen in Lallemand Fjord as well. However, the temperature profile did not show corresponding cold water layers as was seen in the study by Domack *et al.* (1994). Instead it has been suggested that the CDW contributes to undermelt and/or resuspension of particles in front of the ice shelf and that this suspended material creates the mid-water layers (Brandon, 1998).

2.4.3. Underflow

Underflows from inflow directly into the marine environments are considered rare. The difference in density between the sediment plume and the ambient water is most commonly too great to allow for the sediment plume to overcome buoyancy effects and form turbidity currents. In order for the plume to sink the concentration of the suspended sediment must exceed 30-40 kg m^{-3} (Gilbert, 2000). Such conditions are met under certain circumstances. For example, subglacial discharge may increase its sediment load by entraining debris at the efflux or by turbulent mixing at the outlet due to a hydraulic jump

(Mackiewicz *et al.*, 1984). Underflows also form during catastrophic events such as jökulhlaups (Syvitski, 1989) and when remobilization of sediment deposited on sufficiently steep slopes delivers sediment by a variety of gravity flows to more distal marine settings.

2.4.4. Presence of sea ice

The presence of sea ice in the glacimarine environment can either promote or slow water circulation. Circulation is promoted during ice formation when salt is rejected from the freezing ice. The rejection of brine and the cooling of the surface water increase the density of the top layer and extensive mixing takes place (Syvitski and Shaw, 1995; Gilbert, 1983). However, circulation is slowed by the ice as it prevents wind and waves. In addition, as sea ice melts, it forms a stable column at the surface preventing circulation during the melting season.

2.4.5. Particle settling

Suspended sediment entering the marine environment is most often transported as single grains. A dump of mixed grain sizes separates and individual grains fall according to their size. This can take the form of lateral separation where currents work on the sediment. Thus, coarse grains will fall near the source but finer grains may be transported away (Gilbert, 1990).

The settling velocity (v_f) of a falling silt or clay grain can be calculated using Stoke's law:

$$v_f=(g/18\eta)\ (\rho_g-\rho_w)d^2 \qquad (cm\ /\ s)$$

where d is the diameter, g is the gravitational acceleration, η is water viscosity, and ρ_g and ρ_w are particle and water density, respectively. Using this equation, Gilbert (1983) calculated the fall velocities for different sized grains, falling through a 100 m column of saline water, in 0°C. A 14 μm particle takes 12 days; a 4 μm particle takes 146 days, and a 1 μm particle takes 13 years.

There are three processes that cause clumping ("marine snow") allowing particles to settle faster than they would individually: flocculation, agglomeration, and pelletization (Syvitski, 1989; 1991). Flocculation of fine-grained clay particles occurs when the repulsive forces on the surface of the particles are reduced. This process takes place during entrainment of saline water into the freshwater plume. The saline water acts as an electrolyte and the negatively charged surface of the clay mineral connects with a positively charged edge (Syvitski, 1989; Dowdeswell, 1987; Drewry, 1986). Agglomeration is the result of biological interaction with the already flocculated material. Organic detritus attaches to mineral grains by surface tension and organic cohesion (Syvitski, 1989). For example, this can be the incorporation of mineral flocs into phytoplankton matting. Lastly, pelletization takes place where zooplankton ingest mineral and other grains and the resulting faecal pellets sink rapidly to the bottom (Syvitski, 1989).

2.4.6. Tides

Tides create barotrophic currents that move sediment over the sea floor. This process becomes increasingly important during the winter when meltwater input to the marine environment is low (Dowdeswell, 1987). Tides may also influence the position of meltwater plumes and the deposition of sediment from them. Cowan and Powell (1990) found that sediment flux was highest during low tides when turbulence within the plume was lowest. Sorting of sediment occurred as particles settled. The coarse sand and silt settled faster than the finer flocs, resulting in characteristic laminae for each tidal ebb.

2.4.7. Coriolis effect

The Coriolis effect occurs as a result of an apparent force that influences the patterns of sedimentation in fjords. It is caused by the centrifugal effect due to the earth's rotation and causes water with its load of sediment to deflect to the right in the northern hemisphere and the left in the southern (Drewry, 1986). The current eventually flows in a direction approximately parallel to the shoreline (Boggs, 1995) or ,in a fjord, towards one side of the fjord. The general result of this is asymmetric deposits with greater accumulation on the left in the southern hemisphere.

2.5. Sediment redistribution

2.5.1. Mass wasting

Slides, slumps and gravity flows are examples of sub-aqueous mass wasting processes in glacimarine environments. They take place after the initial

deposition of sediment and are caused by gravity acting directly on the sediment. Gravity flows are significant in marine settings as they can transport very large quantities of coarse and fine sediment into deep water (Boggs, 1995). Failure occurs when the shear stress due to the downslope component of gravitational acceleration exceeds the shear strength of the sediment due to internal friction and cohesion between grains. Any primary structures formed from marine sedimentation will thus be destroyed (Dowdeswell,1987).

Ancient slide deposits with volumes in the order of $3\text{-}30\times10^6$ m^3 in several Norwegian fjords suggest that sliding was far more frequent during their main period of sedimentation about 10 000 years ago but several modern slides also prove that mass wasting is still taking place (Aarseth *et al.*, 1989). Sedimentation on the continental slope in the northwestern Ross Sea is primarily by turbidity currents (Anderson *et al.*, 1979).

2.5.2. Iceberg scour

Where the keels of icebergs contact the sea floor, scouring and ploughing of the substrate takes place (Dowdeswell *et al.*, 1993). The fine fraction of the sediment is thus selectively removed (resuspended) and deposited in deeper troughs (Marienfeld, 1992). A significant part of the 500 000 km^2 continental shelf around Greenland has been extensively affected by both scouring and iceberg rafting (Dowdeswell *et al.*, 1994; Dowdeswell *et al.*, 1993). For example, scouring is the most important form of reworking in Scoresby Sund and the average depth of scours is 2-5 m but in extreme cases can be up to 10-12 m

(Marienfeld, 1992). It is significant in water depths <550 m and is most intense between <300-400 m (Dowdeswell *et al.*, 1993). Studies in Antarctica have found that the depth at which scouring can occur depends on the thickness of tabular icebergs. Scouring is normally limited to about 400 m depth but has occurred at 500 m with larger bergs (Powell and Domack, 1995).

2.5.3. Bioturbation

In environments where sedimentation rates are relatively low, benthic organisms may rework and mix sediment. This activity causes the sediment to become homogenised (Dowdeswell, 1987) and any structures that might have been present before, such as laminations or sediment grading, will not be useful for interpretation.

2.5.4. Current activity

At the time of the last glacial maximum, glacial and glacimarine sedimentation were important processes on the Antarctic continental shelf. Today, ice-rafted debris is sparse and siliceous biogenic material dominates. The west Antarctic sectors of the Ross and Weddell seas are characteristic of broad continental shelves where sedimentation takes place well inland of the ice shelf front. The distribution of sediment to the continental shelf is restricted to contour currents that re-work the relict glacial and glacimarine deposits. Marine current velocities, 1 m above the bottom, range from <8 cm/s in shelf basins to 20-25 cm/s on the outer shelf and upper slope (Dunbar *et al.*, 1985; Domack and Anderson, 1983; Anderson *et al.*, 1979).

Currents can also cause already settled material to become resuspended. This has been suggested by significant increase of sediment flux with depth that was collected in sediment traps (Mammone, 1992; Dunbar *et al.*, 1989).

2.6 Summary

The combined influence of sea and glacier ice, fresh and sea water, wind, and biologic activity on sedimentary processes and deposits make the glacimarine environment a complex system. In addition, climate has a control on the amount of sediment released to the environment. The Antarctic Peninsula contains both maritime, sub-polar and polar climate zones but the ability to distinguish these different settings in the sedimentary signal has been difficult due to the influence of all factors that control these processes and because of differences in the physiographic and oceanographic regimes within the same climate zones.

The type of glacier termini determines how sediment is delivered to the water and what sedimentological processes take place in the proximal and distal environment. Glacier ice, icebergs, meltwater streams, and sea ice are sources of terrigenous sediment and most of the biogenic sediment in Antarctica is autochthonous, formed through productivity at the water surface.

Sediment can be transported by overflow, interflow and underflow. Interflow of cold, sediment-laden tongues has been seen in sub-polar fjords of the Antarctic Peninsula and is attributed to basal melting of glaciers. In the polar setting of Lallemand Fjord, interflow was only characterised by sediment-laden

plumes, not cold temperatures as in the cold tongues that have been seen in fjords to the north.

Suspended sediment settles either as single grains or in clumps as a result of flocculation, agglomeration, or peletization. The settling process depends on particle size and is influenced by currents, tides and the Coriolis force. Once settled on the sea floor, the sediment can be redistributed by mass wasting, iceberg scour, bioturbation, and current activity.

A summary of the sedimentary environment in Antarctic Peninsula fjords is presented in Fig. 2.1.

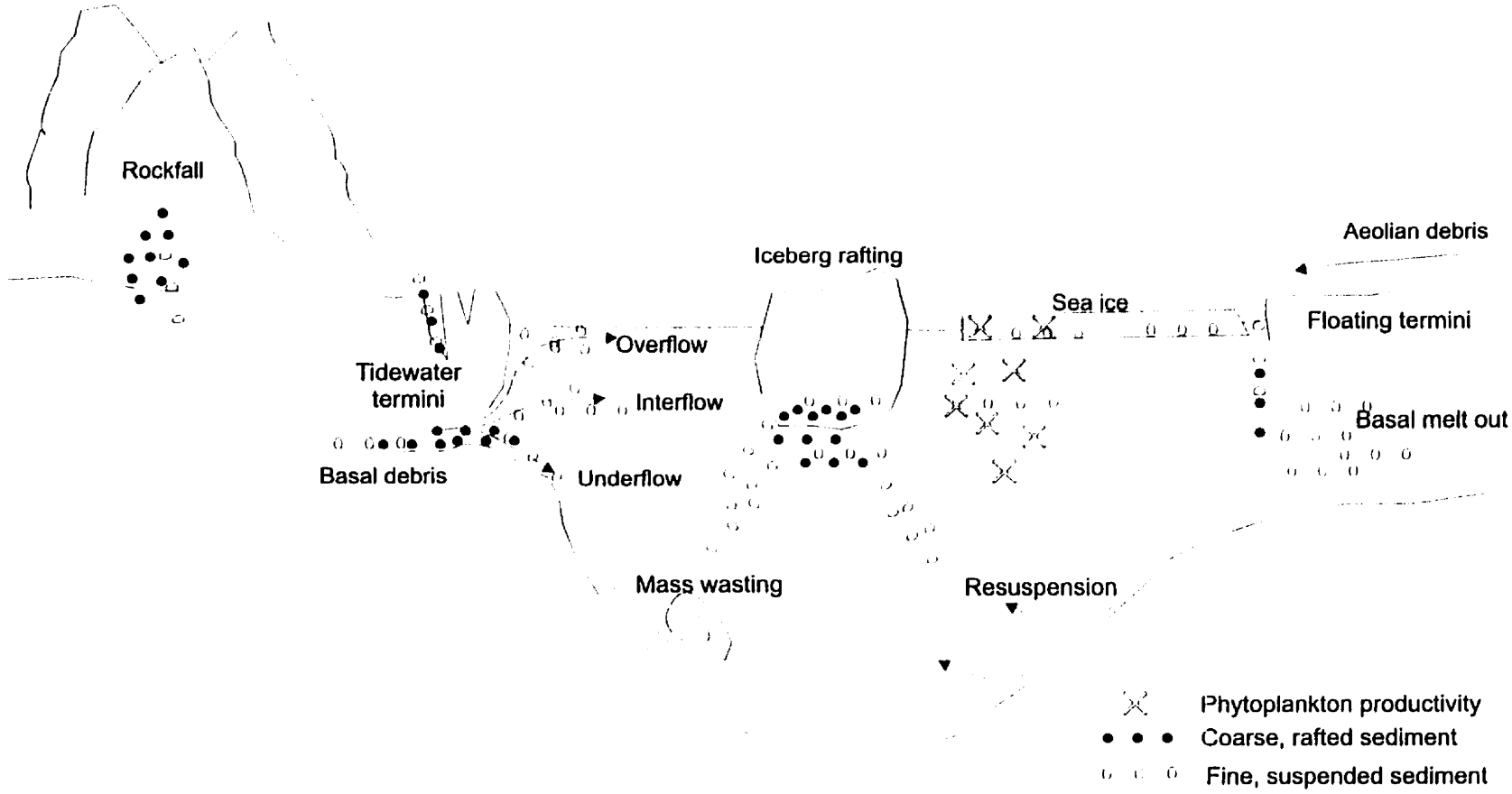

Fig. 2.1 Sedimentation model for a glacimarine environment in Antarctic Peninsula fjords including sediment sources such as glacial ice, aeolian debris, iceberg rafted debris, and redistribution processes such as mass wasting, and resuspension.

Chapter 3: Methods

3.1 Field Methods

3.1.1 Sediment traps

Twelve sediment traps were used in this study. Four of the traps came from Hamilton College, New York (mooring A). The other eight traps were made at Queen's University (moorings B, and C), using a mold borrowed from Dr. R. Dunbar at Stanford University. The original traps used Nalgene bottles as receiver cups attached to the bottom of the fibreglass cones. That design was modified for this study (Fig. 3.1). Instead of using a 500 mL Nalgene bottle at the bottom of the funnel, the top and bottom ends of a Nalgene bottle were cut off and each piece was attached to either end of a clear perspex tube. The diameter of the perspex tube (4.45 cm) was chosen to fit with the Nalgene bottleneck and the length of the tube (30.5 cm) was calculated from the known sedimentation rate at the study site so that one year of sediment accumulation could fit in the tube. The receiver chamber was attached onto the funnel and a PVC pipe was then put over the receiver to protect it while in the water.

There were some differences in the traps made at Hamilton compared to those made at Queen's. The Hamilton traps used a honeycomb mesh with a 10×13 mm opening. The walls between the honeycomb were less than 1 mm thick. The Queen's traps had a mesh of 13 mm wide squares and walls between the squares were 1.5 mm thick. A ring was put on top of each baffle to hold

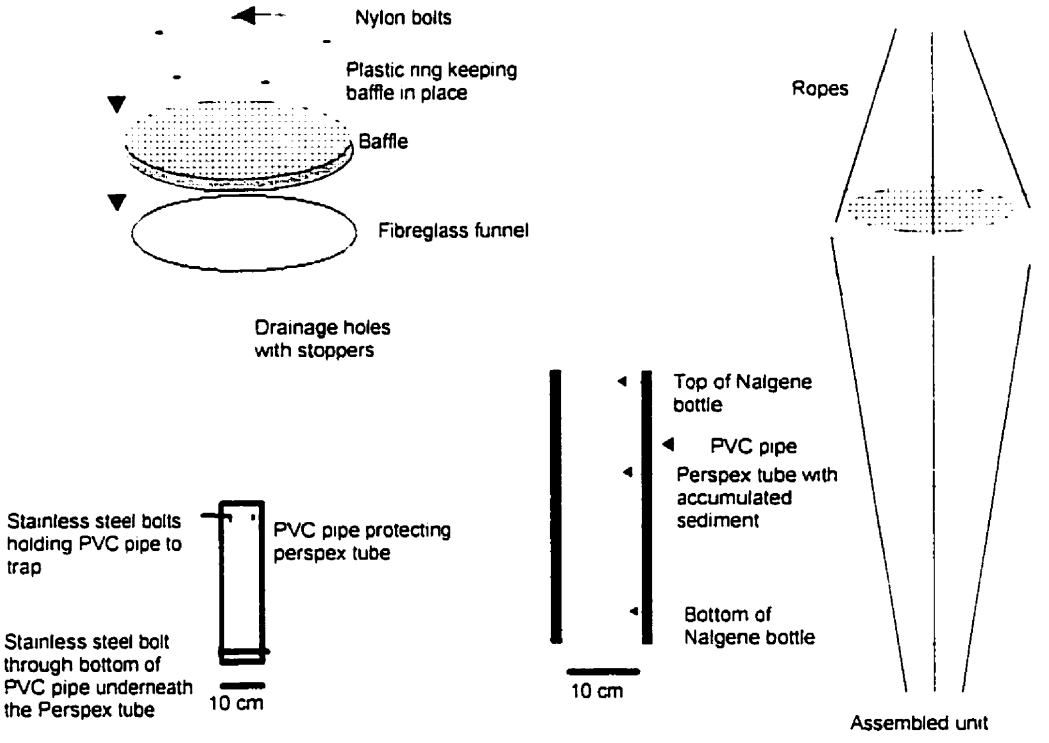

Fig. 3.1 Diagram showing parts and assembly of each sediment trap, detail of the receiver,and an assembled trap with ropes attached.

them in place. There was a difference in width of the ring holding the baffles on the funnel opening which resulted in different collection areas. The area of the Hamilton traps was 0.1555 m^2 and of the Queen's traps was 0.1385 m^2.

Three moorings, each comprising four traps, were used in the study (Fig. 3.2). Two moorings were designed for 600 m depth and placed as close to the ice front as possible. One mooring was designed for 800 m depth and placed away from the ice front. About 50 mL of 0.1 % mercuric chloride was added to each receiver cup to prevent damage to the sediment structures by organisms but due to the way in which the traps were deployed (see below) most of the mercuric chloride was lost. During deployment, the floats were released into the water first and then followed by each trap on a line as the ship steamed slowly forward. When the ship reached the assigned station the main anchor was released and a GPS position was noted for that location. This caused the string to orient vertically as shown in Fig. 3.2. The pick-up line was fed out as the ship continued forward and two smaller weights attached to the pick-up line were released. This insured that the pick-up line would be situated away from the main line.

The traps were deployed on March 3,1998 and retrieved on April 1,1999, thus collecting sediment over 394 days in the fjord. During recovery of the traps, a grappling hook was dragged on the sea floor while the ship followed a pre-planned grid pattern over and around the known mooring position. This pattern

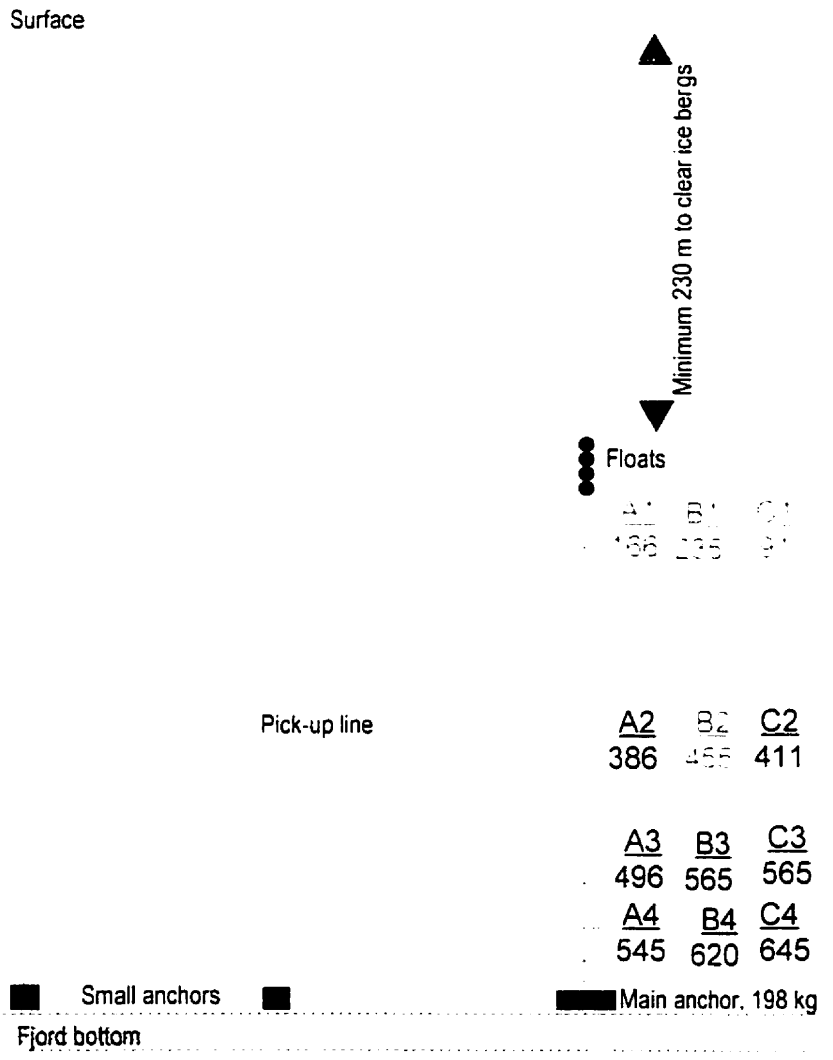

Fig. 3.2 The mooring system used in this study.
Numbers beside each trap show the depth in metres for each trap in the three moorings. In each case the bottom trap was 5 m above the main anchor.
Lost traps are identified in gray.
Mooring locations shown in figure 4.1 .

was designed so that the grapple would drag perpendicular to the pick-up line to snag it. The traps were then slowly lifted up and brought on-board (Fig. 3.3).

The water in the funnel was drained from each trap and kept in a bucket to settle for at least 24 hours. The clear water was decanted and the sediment-laden water filtered through 0.7 μm glass microfibre filters. Each receiver was photographed (Fig. 3.4) and the sediment height was measured. A plug of plastic foam was placed in the top of each core to prevent the sediment from moving during transport back to the laboratory.

A total of eleven sediment traps were recovered in Lallemand Fjord. One trap was lost, two traps were brought up up-side down, and one trap had a broken receiver cup. Thus, out of 12 deployed traps, 8 small receiver cores were returned to the laboratory for analysis.

3.1.2 Other field operations

As part of the science cruise NBP9903 (on board the *Nathaniel B. Palmer)* a SeaBeam swath mapper was used to map the fjord bottom. Parallel transacts across the study area were made so that a complete representation of the sea floor could be made. Since the swath is of constant angle, the distance between the survey transacts depends on the depth of the water, as the width of the swath at the sea floor increases with depth. Isobaths from the SeaBeam survey were fitted to an outline map of the study site to make a bathymetric map of the ice proximal environment (Fig. 3.5).

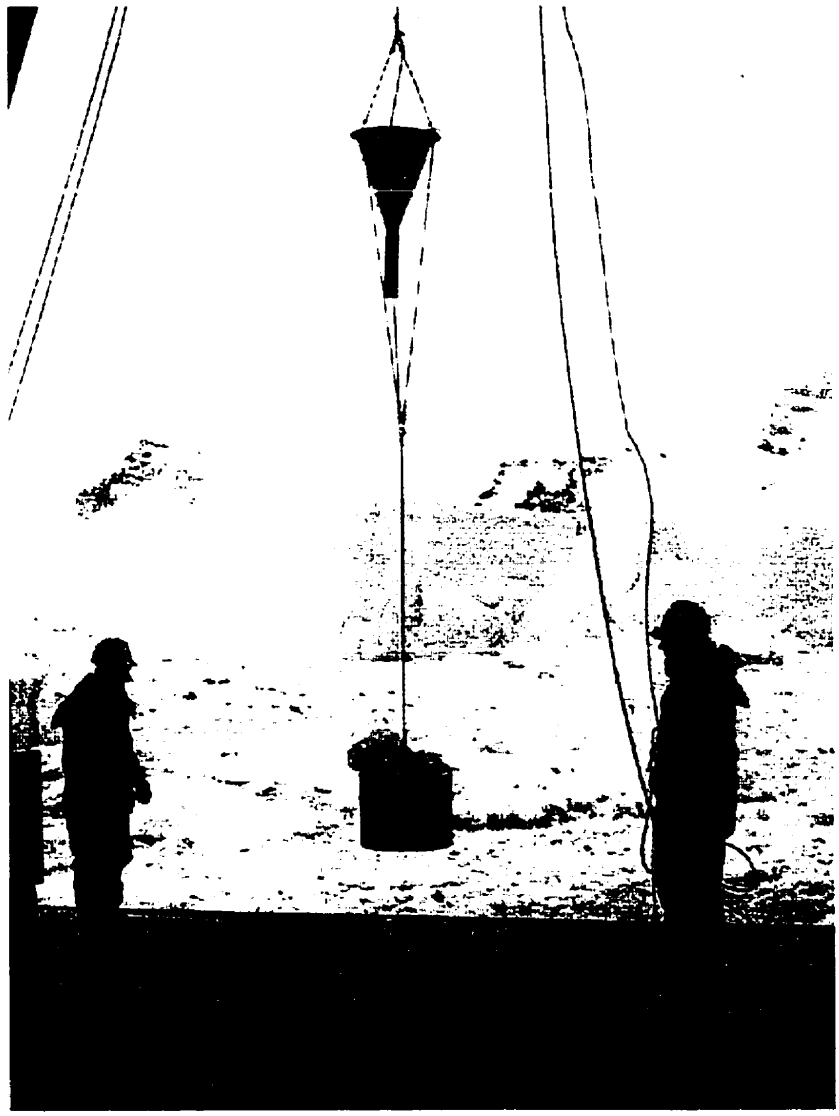

Fig. 3.3 Retrieval of mooring B. Image shows trap B4 coming up.

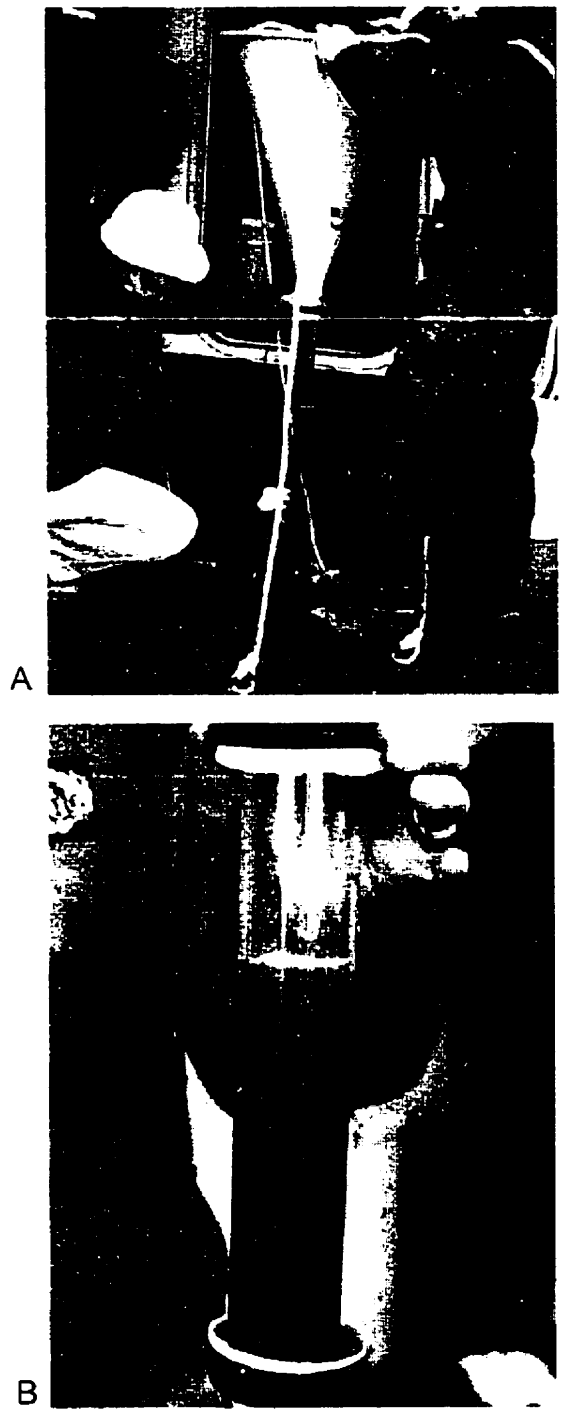

Fig. 3.4 (A) The whole trap assembly during removal of the PVC protective casing and (B) a close-up view of the receiver cup after retrieval.

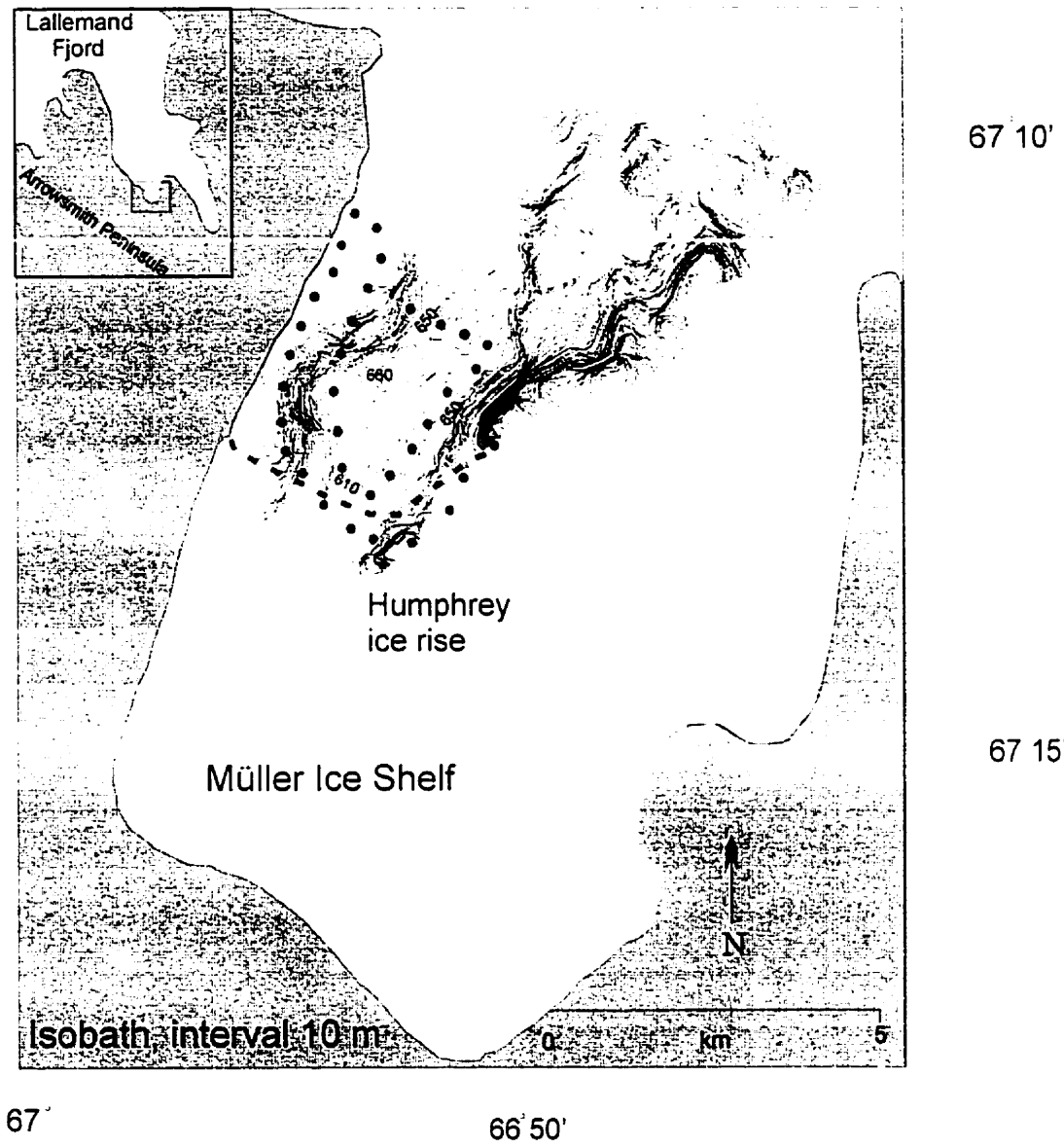

Fig. 3.5
Bathymetric map of the ice proximal environment at the Müller Ice Shelf. Data were obtained on board the *Nathaniel B. Palmer*, in 1999, using a SeaBeam swath mapper. Due to the fan-shaped acoustic transmission the sea floor is mapped for a short distance beneath the ice edge. The apparent conflict with the Humphrey Ice Rise is due to its inaccurately mapped location in earlier surveys.
The dashed line represents the ice edge as mapped in 1995 (Domack *et al.*1995) and the dotted line represents the track line of the acoustic survey along the ice edge in 1998. Trap locations shown in fig. 4.1.

A subbottom acoustic survey was conducted from a 5 m Zodiac inflatable boat, using a Datasonics SBT220 3.5 kHz profiler. A GPS was used to record positions at 2-minute intervals (Fig. 3.5).

Additional work on the two cruises to Lallemand Fjord consisted of sediment coring, seismic surveys, CTD (conductivity, temperature, and depth) casts and dredges as part of the multi-disciplinary and multi-institutional project involving several scientists and their students. The work was in continuation on investigations of the paleoclimatic fluctuations of the Antarctic Peninsula during the Holocene epoch. Samples for paleomagnetism, diatom counts, geochemistry, and physical properties analysis were taken from the sediment. Swath mapping of the ocean floor continued intensely during the 1999 cruise and a large area of the ocean floor in the study area was mapped.

3.2 Laboratory methods

Cores were left vertical for four months in 8 °C to let the sediment settle. During that period, supernatant water was drawn off. The cores were then left to air dry until they reached sufficient consistency such that the sedimentary structures would not be disturbed while lying on their sides. At that point the perspex tubes were split longitudinally. A table saw was used as it seemed to create the least vibration and thus minimised disturbance of the sediment.

3.2.1 Sampling scheme

Each half (referred to as the A-half and the B-half) was used for analysis (Fig. 3.6). The A-half was x-rayed, logged, then sampled for bulk density, total

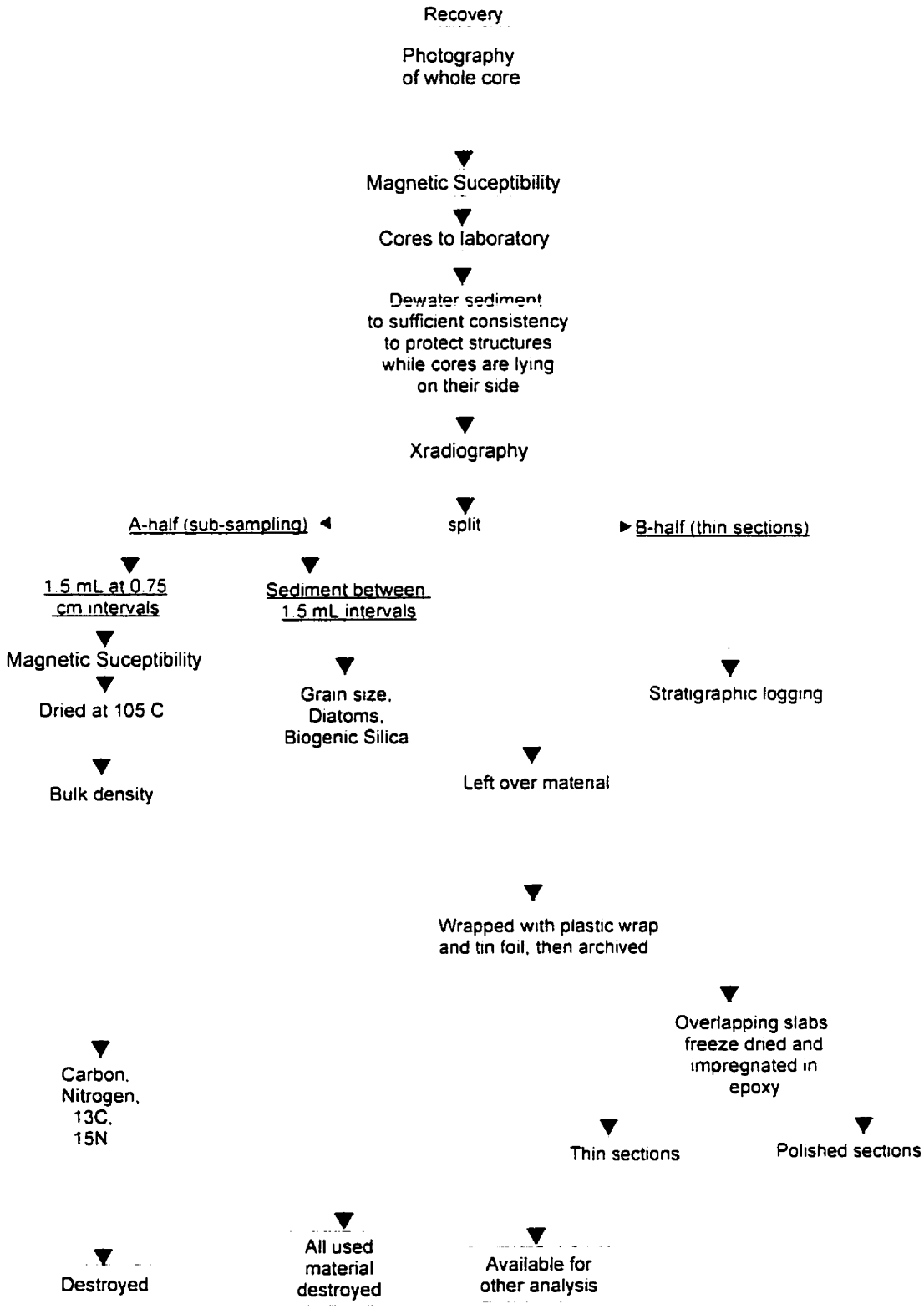

Fig. 3.6 Flow diagram of sampling protocol.

organic carbon (TOC), total nitrogen, δ 15N, $\delta^{13}C$, grain size, and biogenic silica. Samples (volume, V=1.5 mL) were taken with syringes at 0.75-cm intervals but since the syringe covered 1.5 cm there was a 50 % overlap for each sample.

3.2.2 Xradiography

Xradiographs were made for each A-half using a Pickard Industrial x-ray unit. The samples were exposed for 1 minute at 70 kV. Density differences in the sediment, granules, possible burrows from bioturbation, and some sedimentary structures were revealed.

3.2.3 Magnetic Susceptibility (MS)

MS is the ratio of an induced magnetic field in a sample to the intensity of the magnetic field (Ross, 1998). MS was measured twice; first, on-board the ship on the unsplit cores at 2- cm intervals using a Bartington sensor, then in the laboratory where each 1.5 mL sample from the A-half was measured using the internal coil of a Sapphire Instrument SI2B.

3.2.4 Bulk Density, Water content

Each 1.5 mL sample measured for MS was then put in a pre-weighed vial and weighed again to find the wet weight (M_w ,g). The samples were then dried in 105°C overnight and weighed again to determine the dry weight (M_d ,g). The water content was the calculated as:

$$100 \times (M_w - M_d) / M_w$$

and the bulk density was determined as:

$$M_w / V \text{ and } M_d / V.$$

3.2.5 Grain Size Analysis

Grain size was analysed using laser diffraction. This method uses the principle that particles diffract light through different angles depending on size, with the angle of diffraction increasing with decreasing size. A laser beam passes through a suspension and the distribution of diffracted light is analysed by a detector. A Malvern MasterSizer E version 1.2b with 32 detectors and three different lenses that captured different size ranges was used. Most samples only needed the lens that captures a range from 0.1 μm to 100 μm. Two sandy samples required a lens that captured a size range from 1 μm to 1000 μm. Samples were pre-treated with $Na(PO_3)$ solution in an ultrasonic bath to disperse any flocculates in the sediment.

3.2.6 Biogenic Silica (BSi)

Biogenic silica was measured using a wet alkaline extraction method developed by DeMaster (1981) and Krausse *et al.* (1983). 0.1M NaOH was added to dried sediment to dissolve the BSi. Samples were withdrawn from the mixture after 2, 3, 4 and 5 hours and analysed for soluble silica. Total silica analysed is that leached from biogenic sources and clay minerals. However, the BSi dissolves within the first two hours and the silica in clay materials takes longer to dissolve and is thus captured in the later subsamples. Consequently, the BSi can be calculated as the y-intercept of a regression line of weight % silica vs. extraction time. The reproducibility of duplicate samples was 12%.

3.2.7 Thin sections

Twenty five sediment slabs for thin sections were taken over the whole length of each core using a procedure modified from Lamoureux (1994). Each slab was overlapped with the slab above and below. The cut samples were put in a plastic container and submerged in liquid nitrogen to freeze quickly and to avoid ice segregation. Samples were then put in a vacuum chamber and connected to a vacuum pump and a refrigerated vapour trap. After about 30 hours, or when the system reached a pressure of 40-45 μm mercury, resin was added and the samples were put back in the chamber and put under low vacuum to help absorb the resin. Vacuum was slowly increased to avoid disturbance to the sediment by bubbling resin. Then samples were left over night under high vacuum to ensure full absorption of the resin before being put in an oven at 60°C to harden. A thin (3 mm) slice was cut off the surface of each impregnated slab. The new surface was polished with silicon carbide powder using different coarseness in the grit (120, 220, 400). The polished surface was attached to a glass slide using epoxy and cut again so that only a thin section of the original slab was on the glass slide. The new cut surface on the thin section was then ground down until sufficiently thin to distinguish structure in transmitted light.

The purpose of making thin sections was to be able to look at fine scale structures in the sediment. For example, previous studies have found sections of laminations in a core from Lallemand Fjord (e.g. Shevenell *et al.*, 1996). However, the thin section samples were massive and were not used further in the analysis of the traps.

3.2.8 Geochemistry

Sediment samples for isotopic and elemental analysis were dried (60°C), powdered, and 10 to 20 mg weighed into silver foil envelopes. Weighed samples were acidified in situ with 6% sulphurous acid to remove any carbonate phases (Verardo et al., 1990). Sediment samples were analysed for weight % total organic C, weight % total N, and C and N stable isotopic composition using a Carlo Erba NA1500 elemental analyser/Conflo II device and a Finnigan Delta Plus mass spectrometer at Stanford University. Elemental composition was determined by integrating mass 28 and 44 beam intensities (as voltage) on the Delta Plus, calibrated with at least 5 elemental standards analysed during each run. Carbon isotopic reproducibility, as determined by replicate analyses of NBS-21 was 0.08 o/oo (Dunbar, personal communication).

3.2.9 Diatoms

Identification of diatom species in the sediment was done at Colgate College, NY. This was only for the purpose of identifying what species were in the samples, it was not a formal count for diatom concentrations.

3.2.10 Total flux

The total flux in weight was calculated using the formula:

(Volume of sediment × mean bulk density) / collection area of trap / 394 days

The total flux in thickness was calculated by determining the concentration factor between the baffled trap opening and the area of the cross section of the

perspex reservoir (area of trap opening / area of reservoir opening). Then dividing the height of the flux in the trap with the concentration factor).

Chapter 4: Sediment trap records of transport and deposition adjacent to the Müller Ice Shelf, Lallemand Fjord, Antarctic Peninsula

Abstract

Lallemand Fjord (67°S , 66°W) contains the Müller Ice Shelf (MIS), the most northern ice shelf on the western side of the Antarctic Peninsula. The fjord has an ice drainage area of about 1290 km^2 and the ice shelf itself is about 80 km^2. The mean annual temperature is -5°C and it is suggested that this is the northern limit for ice shelves in the Peninsula, making the MIS sensitive to temperature changes. The MIS formed during the Little Ice Age but is now retreating and has met its minimal extent.

Sediment traps were deployed from March 1998 to April 1999. Three moorings with four traps each were deployed at 0.6, 0.4, and 3.7 km from the ice shelf, in 550, 625, and 650 m of water, respectively. Eight traps were recovered. Sediment fluxes ranged from 1.19 to 2.34 mm a^{-1}. The higher flux possibly resulting from current transportation. Sediment is mainly composed of silt and clay with low biogenic silica content (~3-4%) and low carbon content (<2%). Temporal variation in sedimentation was found in both biogenic and siliclastic material. Layers of coarse material at the top and bottom of the records may represent aeolian or ice-rafted debris from autumn 1998 and summer 1999. Biogenic silica shows subtle peaks near the top and bottom, indicating possible productivity peaks from the spring seasons. These results relate to the sedimentary environment at the MIS as interpreted from previous sedimentologic and oceanographic data. For example, sediment fluxes from cores have been estimated to be 1-2 mm a^{-1}. Mid-water sediment transport of suspended particulate matter has been observed at the ice shelf. Deposition of coarse material in proximity to the ice shelf and increasing amounts of ice-rafted debris away from the ice shelf have been seen in sediment cores.

4.1. Introduction

Special interest in ice shelf environments has developed from observations of their apparent sensitivity to climate change. Rapid disintegration of ice shelves such as the Wordie, Wilkins, Prince Gustav Channel, and the Larsen Ice Shelves in the Antarctic Peninsula (AP) has been related to a recorded 2.5°C warming trend over the past 50 years in the region (Vaughan and Doake, 1996; Skvarca, 1993; Doake and Vaughan, 1991) . At the same time there have been changes observed in sea-ice extent (de la Mare, 1997), the duration of the summer melt season (Ridley, 1993), and the location of penguin nesting sites (Emsile *et al.*, 1998) in the region.

Ongoing research seeks to understand if these changes are mainly caused by anthropogenic activity, or if these are normal cycles in the climate regime of the region. The character and composition of glacimarine sediment have been studied to serve as an indicator of the environmental setting upon deposition. One important type of site has been the ice-proximal setting in fjords since these sediments might indicate past fluctuations of the ice-shelves in the AP.

One site for such studies has been the Müller Ice Shelf (MIS), in Lallemand Fjord, the most northern ice shelf in the AP. As part of continued sedimentological studies at this site, sediment traps were deployed to collect sediment during one year and these results were compared with those found in sediment core analysis. These studies have found down-core variability in

sedimentary properties that are believed to be caused by changes in the position of the ice shelf. For example, there is a decrease in well-sorted sand with increasing distance from the ice shelf and a corresponding increase in organic carbon. Down-core sediment appears to reflect this trend as well. Sections of well-sorted sand replace sections of sediment high in organic matter and it has been suggested that these changes represent fluctuations in the ice shelf position (Domack and McClennen, 1996; Stein, 1992). This study used sediment traps to collect material over a one year period at the MIS and the results were compared with previous sediment core studies.

4.2. Study Site

The MIS is situated near the head of Lallemand Fjord on the western side of the Antarctic Peninsula at 67°S, 66°W (Fig. 1.1). It formed in the Little Ice Age (Domack *et al.*, 1995) but is currently retreating (Ward, 1995; Stein, 1992), and is now at its minimum recorded extent (Vaughan and Doake, 1996). Its continued presence has been attributed to the protective setting in the fjord (Shevenell *et al.*, 1996) and the fact that the ice shelf is pinned to the Humphrey ice rise (Fig 1.1).

Monthly mean temperatures were measured at Rothera (67° 34' S, 68° 08' W). Temperatures recorded between 1976 and 2000 show inter-annual variations that are especially large during winter (Fig. 1.2). Significant correlation between air temperature and sea ice extent has been found in the AP (King and Turner, 1997) and it is possible that the region is sensitive to even small changes in sea ice extent. Fast ice in Lallemand Fjord can be persistent well into the

summer, whereas in some years the fjord may be ice-free in December (Shevenell *et al.*, 1996).

Circumpolar Deep water (CDW) contributes to the melting of the bottom of the MIS (Domack and Ashley, in preparation) which releases sediment that becomes suspended in mid-water layers. However, no apparent meltwater plume has been detected and it is therefore difficult to know how much basal melt takes place. The suspended sediment might also reflect resuspension by the upwelling CDW in front of the ice shelf (Brandon, 1998).

4.3. Methods

Twelve cone-shaped fibreglass sediment traps were used in this study. Eight traps were made at Queen's University and four traps were provided by Hamilton college. The Hamilton traps had a baffled opening of 0.1555 m^2 and the Queen's traps of 0.1385 m^2. The Perspex reservoirs holding the sediment were 0.0016 m^2 in cross-section (4.45 cm in diameter) and 0.3 m long, representing a concentration factor between the mouth of the trap and the reservoir of 100.2 and 89.3 respectively. Three moorings (A, B, and C) were made and each had four traps with the bottom trap anchored 5 m above the sea floor and the others spaced out in the water column. The moorings were set in (A) 550 m, (B) 625 m, and (C) 650 m of water depth, 0.6 km, 0.4 km, and 3.7 km from the ice edge, respectively (Fig. 4.1). The traps were deployed on March

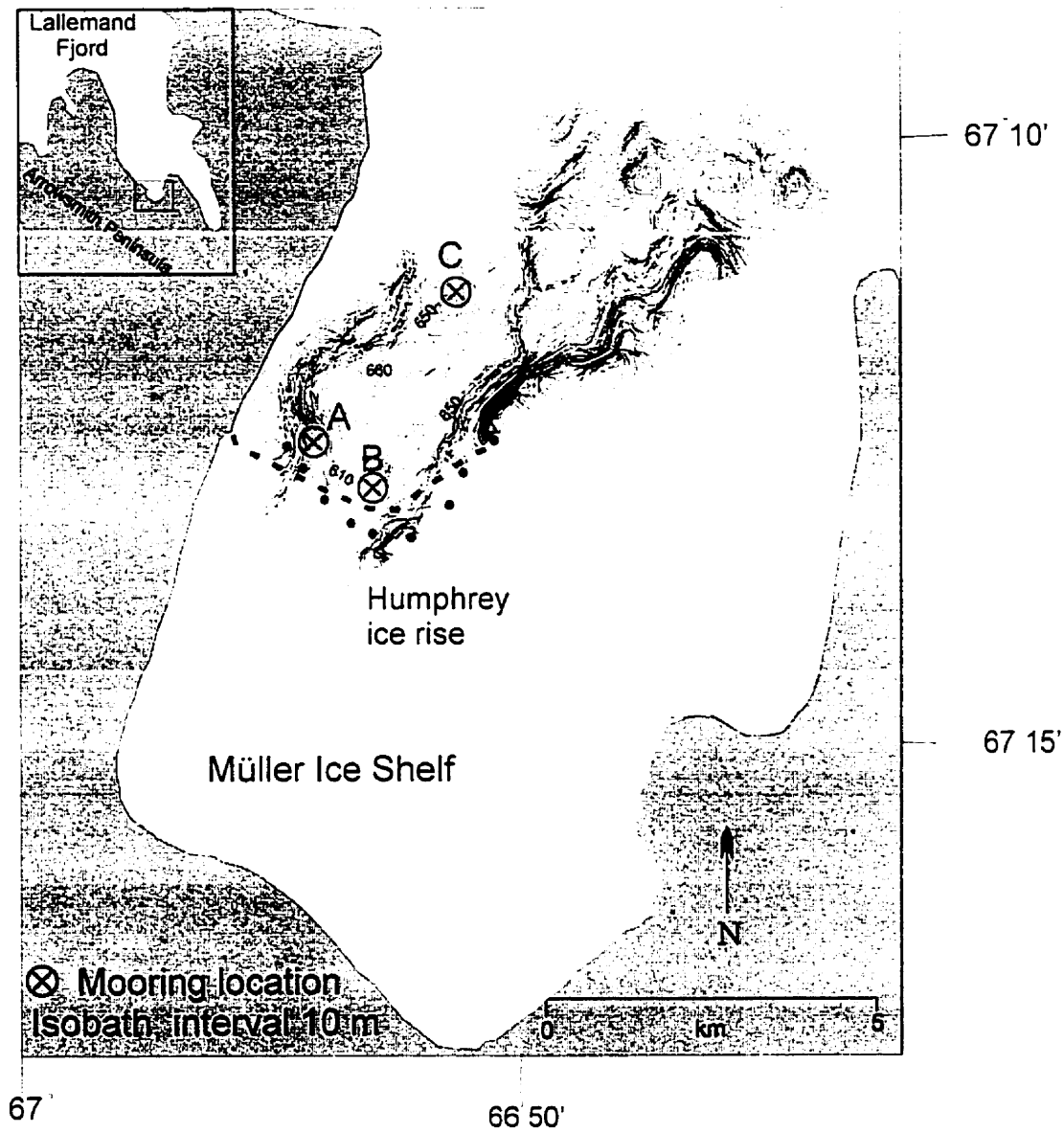

Fig. 4.1 Location of mooring A, B, and C. See fig. 3.5 for discussion of bathymetry in relation to the ice front and coast. The dashed line indicates the ice edge as mapped in 1995 (Domack *et al.* 1995) and the dots indicate the track line of the acoustic survey along the ice edge in 1998 (Gilbert, personal communication).

3,1998 and retrieved by grappling in April 1, 1999, giving 394 days during which sediment was collected.

Upon retrieval, the traps were slowly lifted up and brought on-board. The water in the funnel of each trap was kept and left to settle for at least 24 hours. The clear water was decanted and the sediment-laden water was filtered through 0.7 μm glass microfibre filters. Each receiver was photographed and the height of the column of sediment was measured. Eight traps provided useable records and were returned to the laboratory.

After the reservoirs were brought back to the laboratory, they were left for four months to air dry. During this time the supernatant water was drawn off the top of the sediment. Once the sediment had reached a consistency that allowed the reservoirs to be put on their side without disturbing the sediment, the reservoirs were cut longitudinally using a table saw.

Each half (referred to as the A-half and the B-half) was used for analysis. The A-half was x-rayed and logged, then sampled for bulk density, magnetic susceptibility, total organic carbon (TOC), total nitrogen (TN), $\delta^{13}C$, $\delta^{15}N$, grain size, and biogenic silica. Samples of volume 1.5 mL were taken using syringes at a 0.75 cm interval but since the syringe covered 1.5 cm, all samples were staggered and there was a 50% overlap between each sample.

Xradiographs were used to count the coarse-grained fraction of the sediment and to determine the ichnofabric classification of the sediment. The coarse-grained fraction was found by counting all coarse grains larger than 1 mm

diameter within each 6 mm interval of the core (cf. Grobe, 1987). The method for ichnofabric classification followed Gilbert *et al.* (1998) as modified from Droser and Bottjer (1986). This qualitative classification describes the degree of lamination in the sediment from strongly laminated to unlaminated. Samples for water content and bulk density were dried in 105°C over night. Magnetic susceptibility was measured using a Sapphire Instruments SI2B. Grain size was measured on a Malvern MasterSizer E version 1.2b. Sediments was sonicated and pre-treated with $Na(PO_3)$ to disperse flocculation. Biogenic silica (BSi) was measured using a wet alkaline (0.1M NaOH) extraction method developed by DeMaster (1981) and Krausse *et al.* (1983). Thin sections were made using method modified from Lamoureux (1994). Freeze drying was used instead of acetone to dewater the sediment. Resin was then added to the samples and they were put under vacuum to ensure full absorption of resin into the sediment. However, the thin sections were not used further in the study as they did not show any sedimentary structures.

4.4. Results

The trap results are presented for each trap temporally through the collection period, and spatially by comparing results among traps. Table 4.1 lists the fraction of sediment recovered in the supernatant water in relation to the amount captured in the traps.

Table 4.1 The fraction of sediment in supernatant water to sediment collected in the traps (H=Hamilton trap, Q=Queen's trap).

Trap	Depth (m)	Wt. of sediment in traps (g)	Wt. of sediment in funnel (g)	Fraction (%)
A2 (H)	386	97.048	5.101	5.25
A3 (H)	496	111.411	7.572	6.70
A4 (H)	545	128.042	0.517	0.40
B3 (Q)	565	129.185	0.483	0.04
B4 (Q)	620	175.1493	6.687	3.82
C2 (Q)	411	105.337	0.825	0.78
C3 (Q)	565	245.881	0.103	0.04
C4 (Q)	645	178.473	1.667	0.93

4.4.1 Temporal Variation

A2 (Fig. 4.2) is 11.9 cm long and consists of black (5Y 2/1) fine to medium silt. It is unlaminated in the top 2.25 cm and bottom 3 cm and very faintly laminated between. It has only two areas where some coarse material was deposited: near the top around 1.5 cm then in the middle at about 7.5 cm; there are a couple of granules in between. The sand component is 5% or less, with the largest amounts in the lower section of the sample. Clay and silt are about 45% and 55%, respectively, and show little variation through the sample. Bulk density ranges from 0.4-0.7 g/cm^3 and higher magnetic susceptibility coincides with peaks in bulk density. Biogenic silica ranges from 2.8 to 5.8 % with generally highest amounts at the top and bottom of the core (Fig. 4.3). Nitrogen and carbon contents are low. They are both higher at the bottom and carbon is slightly higher at the top but the middle is low and constant in both. The $\delta^{15}N$ and $\delta^{13}C$ are lowest at the top and bottom and stable in the middle. The carbon/nitrogen ratio has a peak at the top and decreases gradually towards the bottom.

A3 (Fig. 4.4) is 12.9 cm and consists mainly of very dark grey (5Y 3/1) sediment with streaks of black (5Y 2/1) in the middle section. It is classified as very faintly laminated throughout except between 6.8-11.2 cm where it is faintly laminated. It has some more areas of coarse sediment than A2 and they are mostly situated in the bottom half. The bulk density increases from 0.48-0.68 g/cm^3 in the first 3.75 cm then varies between 0.43 and 0.72 g/cm^3 with low values at 5.25 and 8.25 cm. This pattern is reflected in the MS as well. The

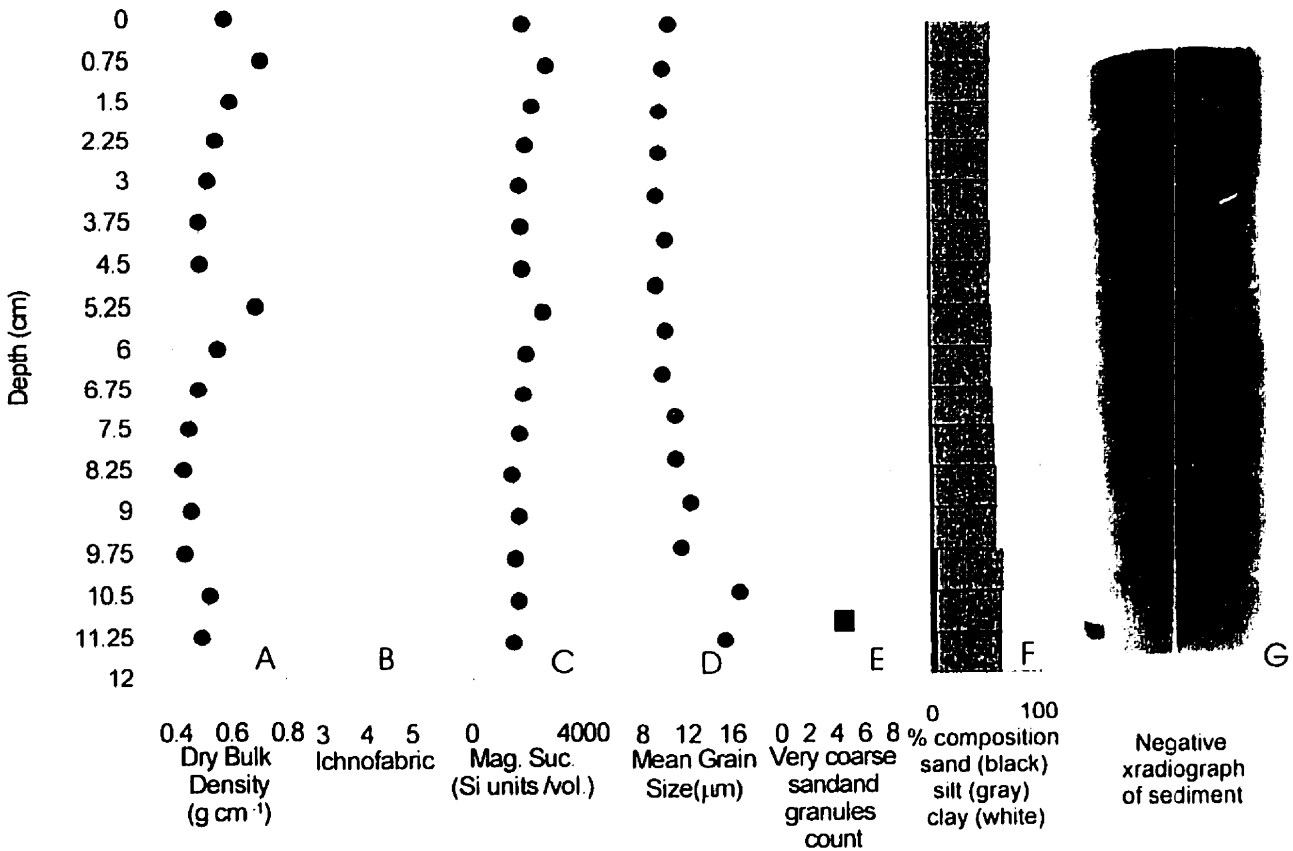

Fig. 4.2 Results of analysis on physical properties of sediment collected in trap A2: (A) bulk density, (B) Ichnofabric classification where 3 is faintly laminated, 4 is very faintly laminated and 5 is unlaminated, (C) magnetic suceptibility (D) mean grain size, (E) coarse grain count of grains >1 mm, (F) composition sample grain sizes, (G) negative xradiograph in which darker tones represent less transmission of the x-ray beam. ■ = clasts > 4 mm

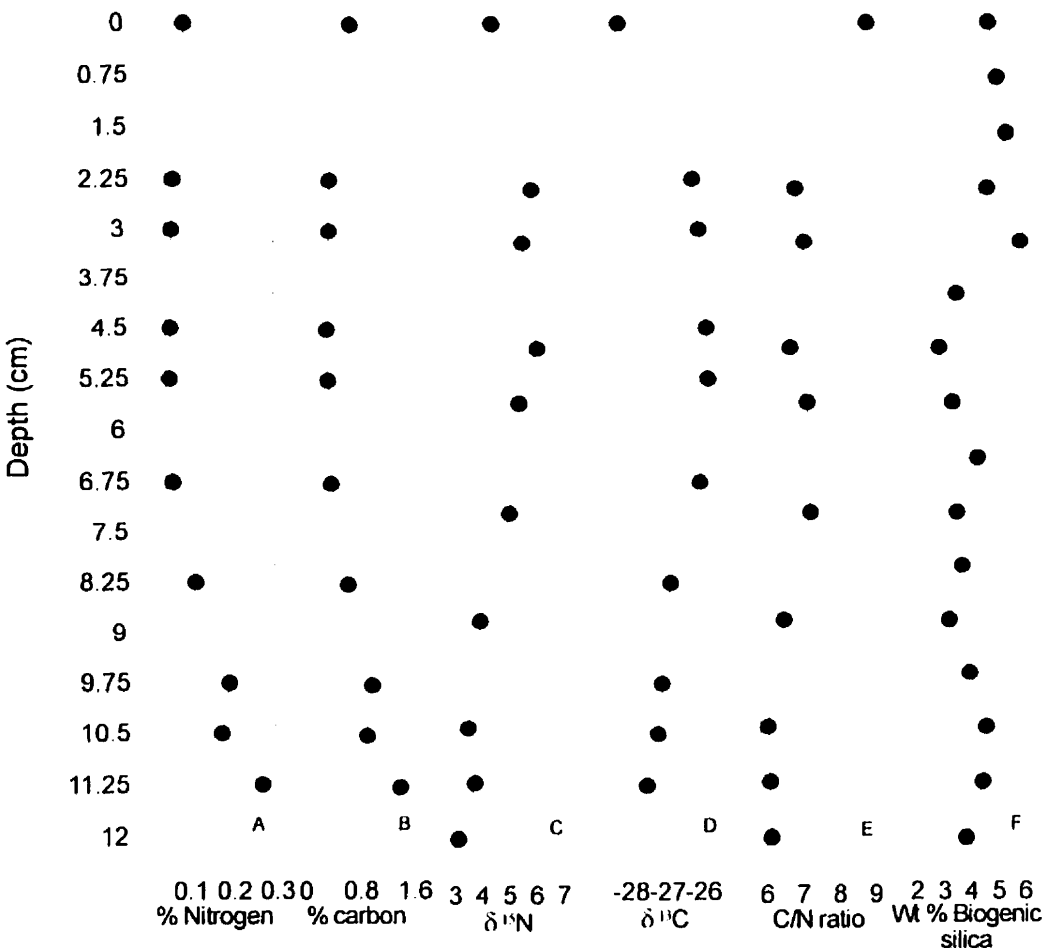

Fig. 4.3 Results of analysis of biogenic properties of the sediment collected in trap A2. (A) % nitrogen, (B) % carbon, (C) isotopic nitrogen (D) isotopic carbon (E) the carbon/nitrogen ratio, (F) and the weight percent biogenic silica.

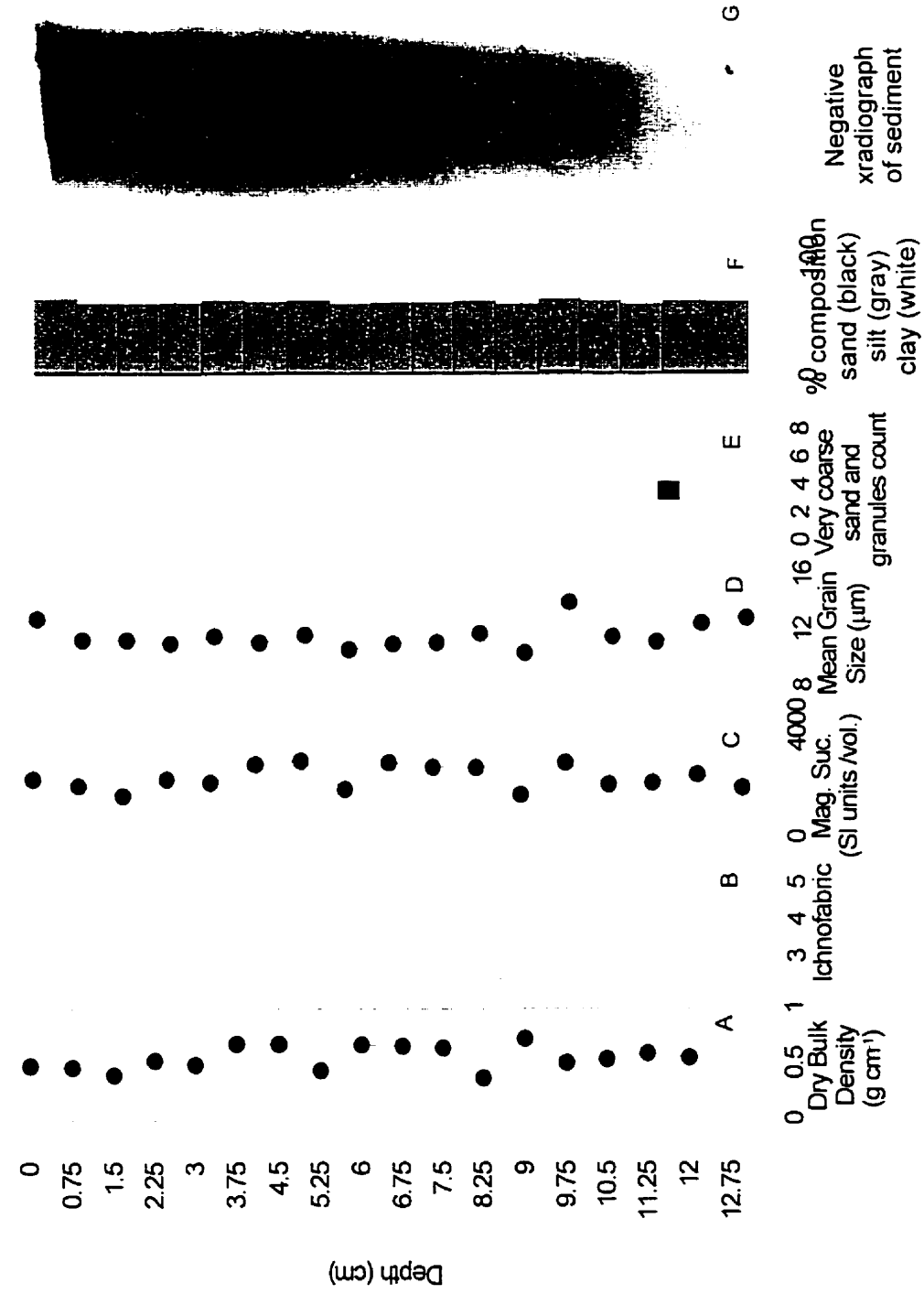

Fig. 4.4 Results of analysis of sediment collected in trap A3.
See Fig. 4.2 for information on each graph.

mean grain size is around 12 μm and peaks at 9 cm with a larger content of sand. The sediment is composed of about 38% clay, 60% silt and 2% sand. Biogenic silica lies between 2.4 and 5.8% with the higher values at top and bottom (Fig 4.5). Nitrogen and carbon contents are slightly increased at the bottom, constant through the middle and carbon has another small peak at the top. The $\delta^{15}N$ is low at the top and bottom but rises in the middle. The $\delta^{13}C$ is lowest at the top but stable throughout. The carbon/nitrogen ratio peaks at the top and remains stable below to the bottom. A4 (Fig. 4.6) is 13.4 cm long and mottled with very dark grey (5Y 3/1) and black (5Y 2/1). It has coarse material throughout but higher concentrations in the bottom half. Most of the core is faintly laminated but the top 1 cm and the bottom 3.5 cm are unlaminated. It has a bulk density between 0.8 and 0.4 g/cm^3 with peaks at 0.75, 1.5, and 8.25 cm. This same pattern is reflected in the MS. The mean grain size fluctuates around 12 μm and the sediment composition is about 44% clay, 54% silt, and 2% sand. Biogenic silica is between 2.5 and 6.4 % with highest peaks at 0.75 cm and 8.25 cm (Fig. 4.7). Nitrogen and carbon peak at the bottom, then remain fairly low and stable to the top. Both $\delta^{15}N$ and $\delta^{13}C$ are fairly stable throughout and decrease slightly at the bottom. The carbon/nitrogen ratio varies slightly throughout but has slight peaks at top, middle, and bottom.

B3 (Fig. 4.8) is 13.1 cm long and is mottled with very dark grey (5Y 3/1) and black 5Y2/1). Remnants of an organism was seen in the trap receiver upon retrieval. It has coarse material throughout but with a high peak at around 12 cm. The top 6 cm are unlaminated and the rest is classified as faintly laminated.

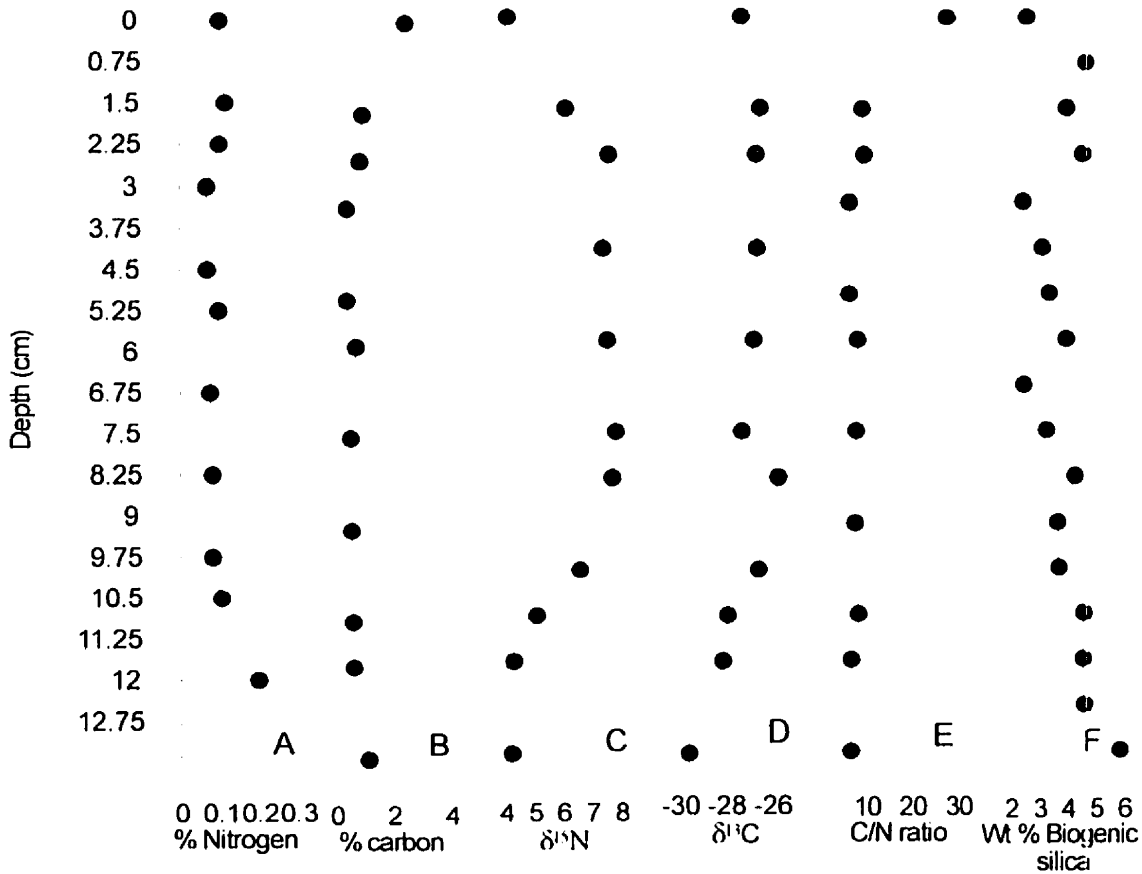

Fig. 4.5 Results of analysis of biogenic properties of the sediment collected in trap A3. See figure 4.3 for information on each graph.

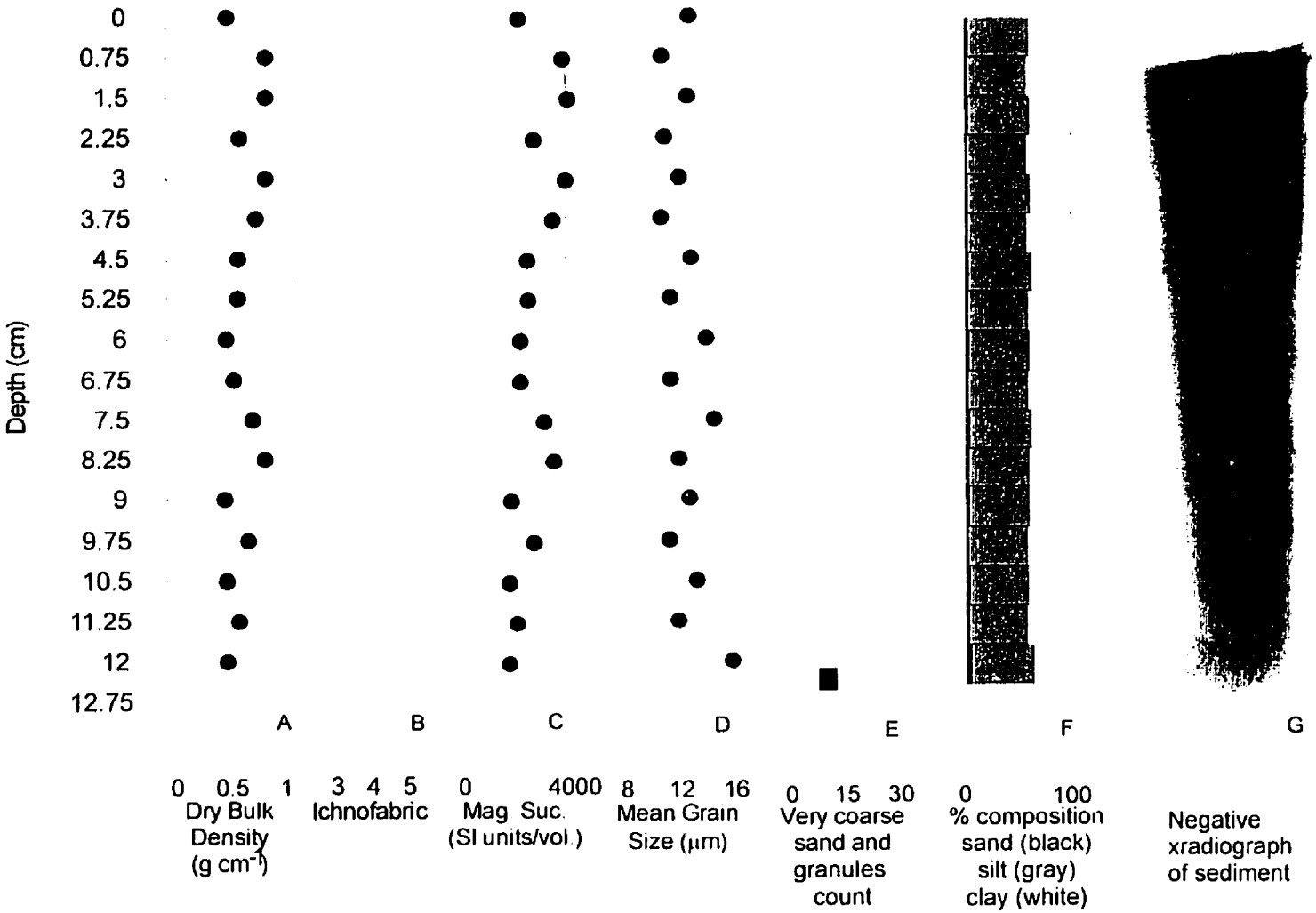

Fig. 4.6 Results of analysis of sediment collected in trap A4. See Fig. 4.2 for information on each graph.

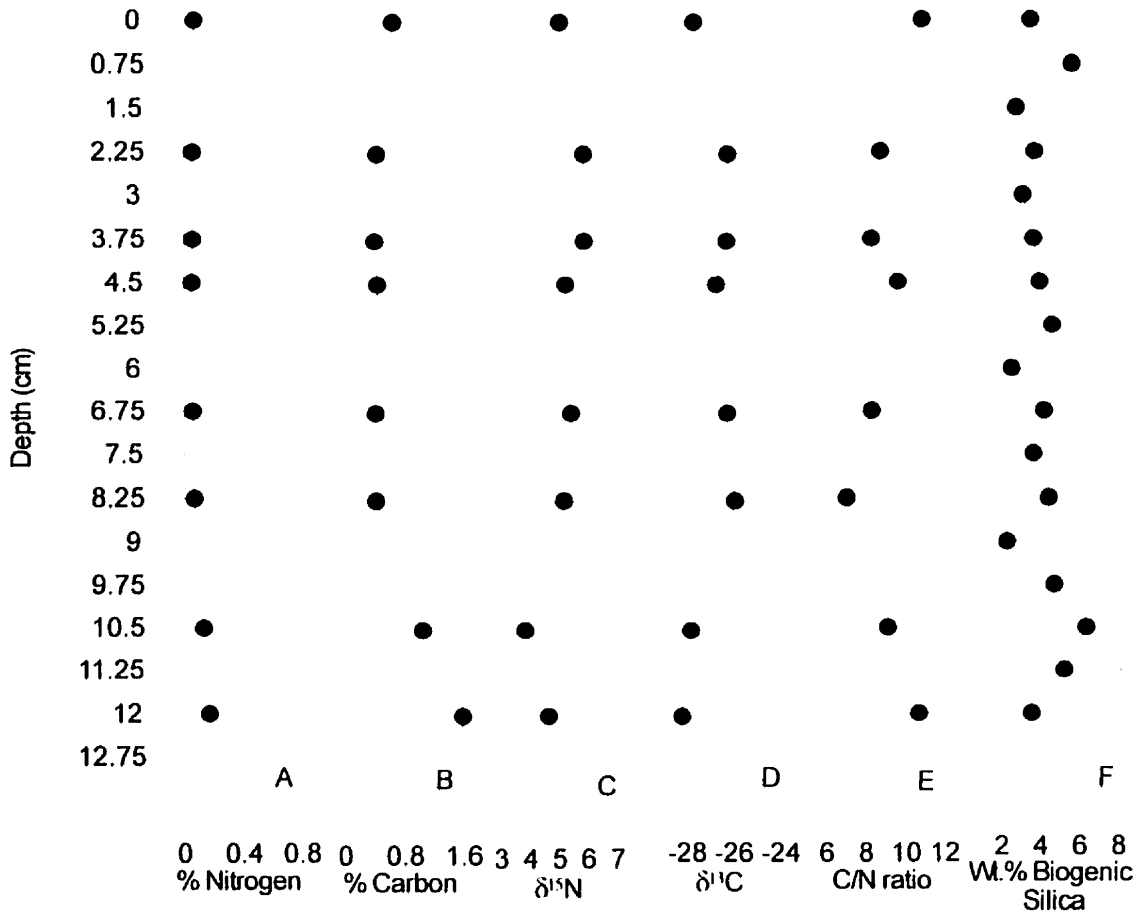

Fig. 4.7 Results of analysis of biogenic properties of the sediment collected in trap A4. (A) % nitrogen, (B) % carbon, (C) $\delta^{15}N$, (D) $\delta^{13}C$, (E) the carbon/nitrogen ratio, and (F) the weight percent biogenic silica.

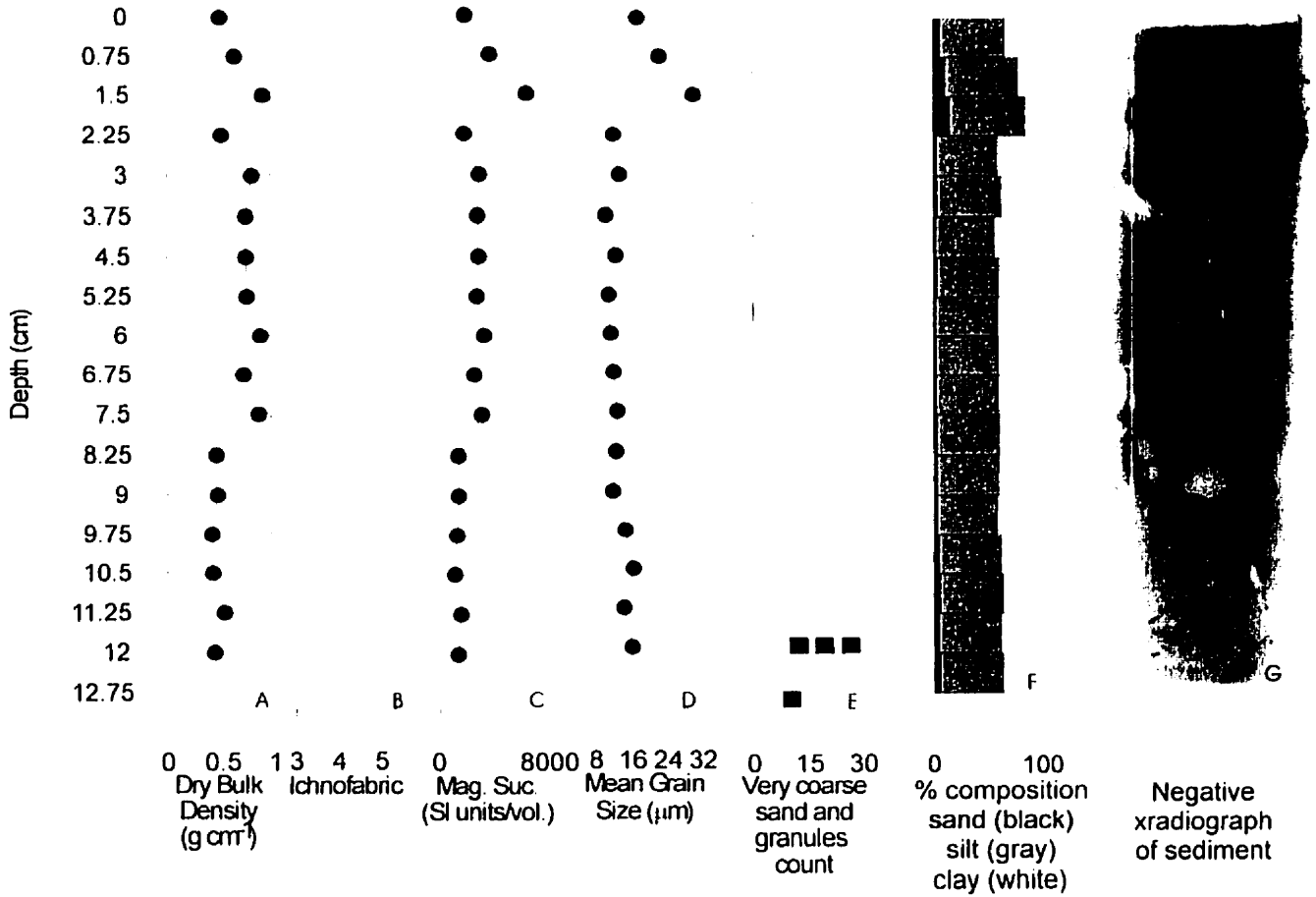

Fig. 4.8 Results of analysis of sediment collected in trap B3. See Fig. 4.2 for information on each graph.

The bulk density lies between 0.7 and 1.3 g/cm^3 in the first 7.5 cm then decreases to about 0.65 g/cm^3 in the bottom section. The variations in bulk density are reflected in the MS as well. The mean grain size is about 17 μm except at the peak in the top 1.5 cm. The volume % composition is in general 42, 55, and 3 % clay, silt and sand, respectively. But near the top sand increases to 11 and 15 % and at a small peak at the bottom 3 cm sand is about 5%. Biogenic silica ranges from 4-6%, peaking at the top and bottom (Fig. 4.9). Nitrogen and carbon peak at the top and bottom. Nitrogen stays fairly low and stable in the middle, whereas carbon has another peak in the middle. $\delta^{15}N$ and $\delta^{13}C$ have lows at the top and bottom and carbon also has a low in the middle. The carbon/nitrogen ratio is stable throughout except in the middle where it has one peak.

B4 (Fig.4.10) is 14.3 cm long with mottled sediment in very dark grey (5Y 3/1) and black (5Y 2/1). It has coarse material throughout but with definite peaks around 1.5 cm and 11.25 cm. The whole core is unlaminated and has burrows. Remnants of organisms were seen in traps upon retrieval. Bulk density ranges between 0.5 and 1.3 g/cm^3, with a peak at 4.5 cm. The MS is slightly different from the other cores and doesn't have the strong peak at 4.5 cm but increases more steadily to about 5.25 cm then follows the same pattern as the bulk density. The mean grain size is in the silt class but varies more in this core than the other cores. It peaks at 3-3.75 cm and 11.25 cm. It has a low at 1.5-2.25 cm and decreases steadily from 4.5 to 9.75 cm. The % composition is in general 40%, 57% and 3% clay, silt and sand sized particles. At the peaks it

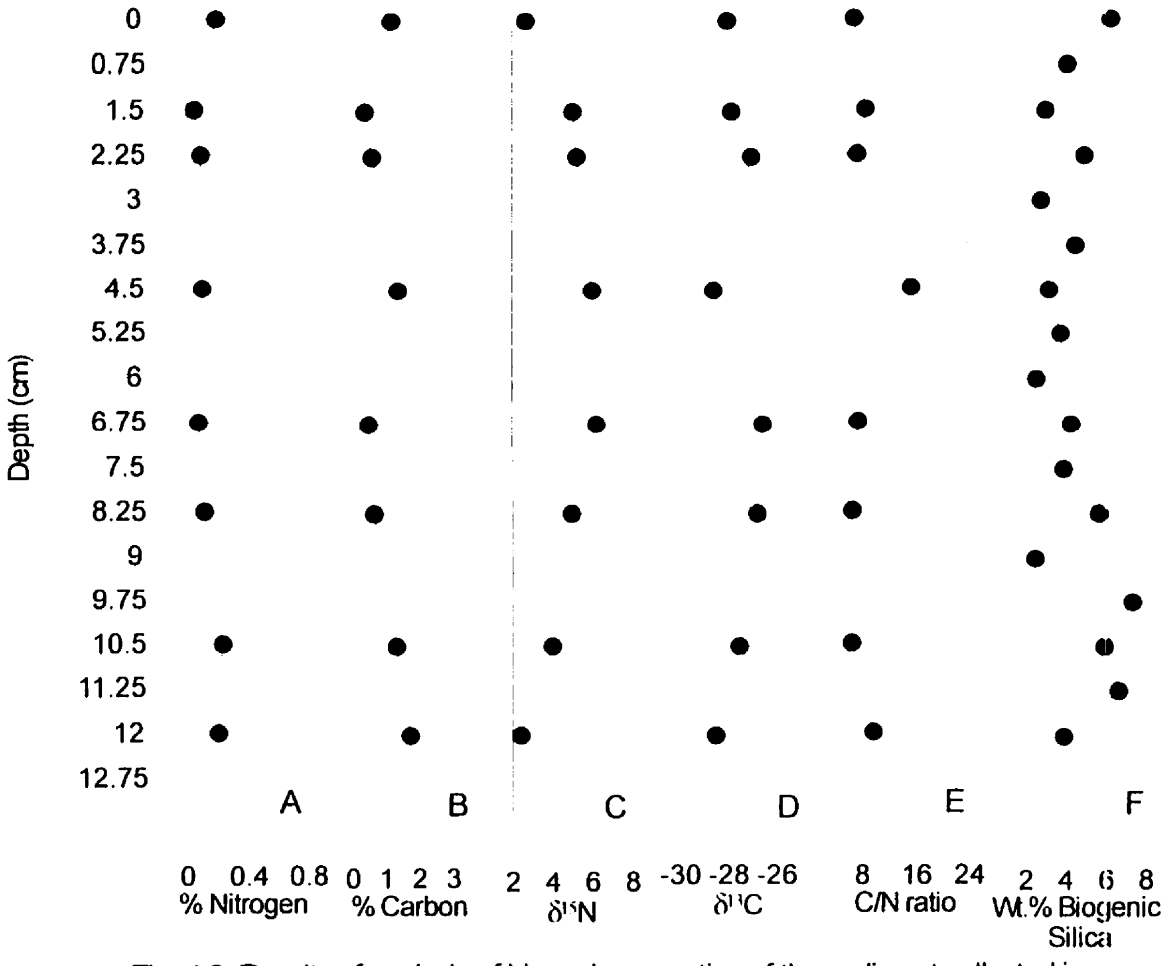

Fig. 4.9 Results of analysis of biogenic properties of the sediment collected in trap B3. (A) % nitrogen, (B) % carbon, (C) $\delta^{15}N$, (D) $\delta^{13}C$, (E) the carbon/nitrogen ratio, and (F) the weight percent biogenic silica.

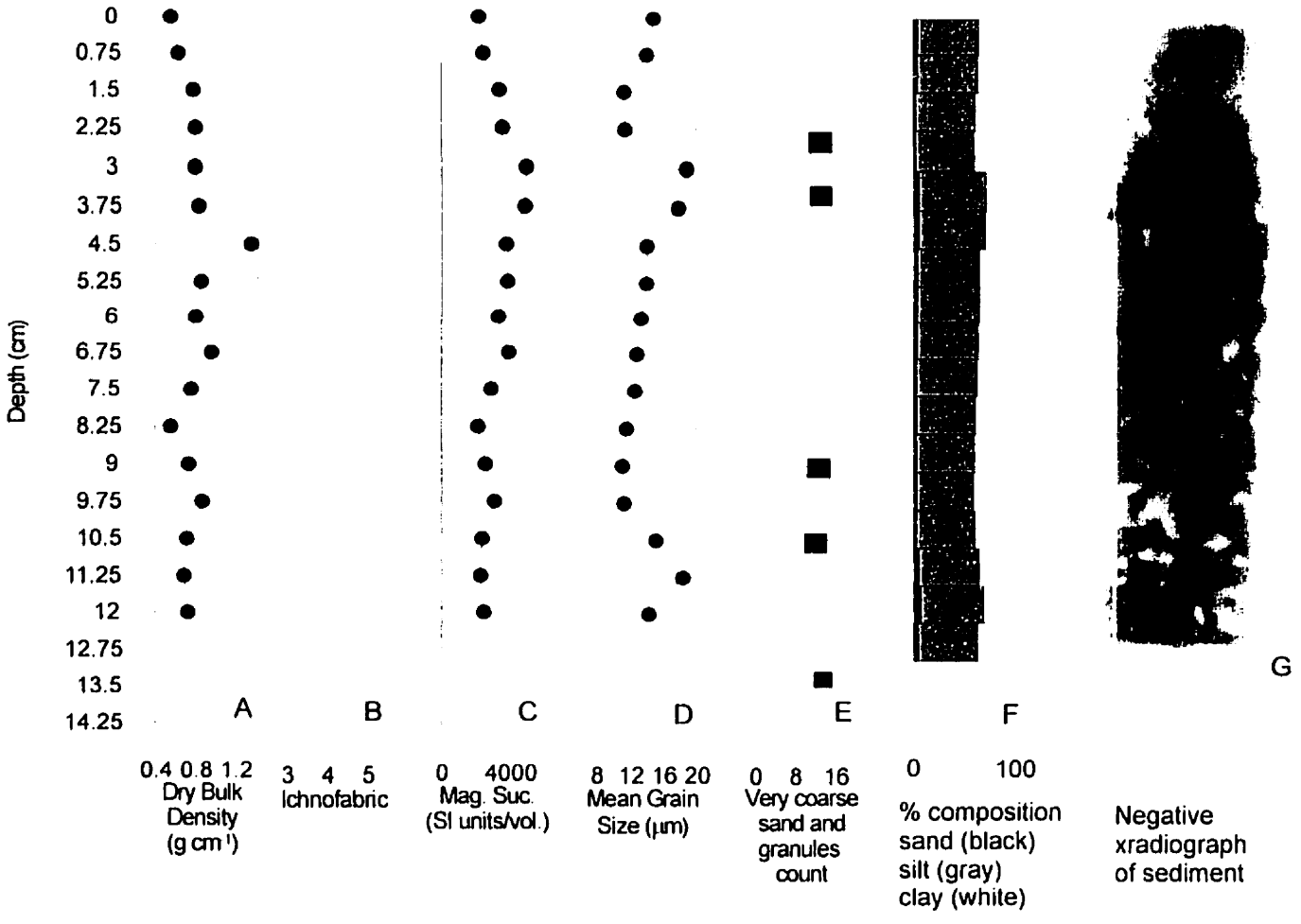

Fig. 4.10 Results of analysis of sediment collected in trap B4. See Fig. 4.2 for information on each graph.

changes to 34%,61%, and 5% at the top peak and 39%, 55% and 6% at the bottom peak. Biogenic silica ranges from 1.3-5.3 % with highs at top and bottom (Fig. 4.11). Nitrogen and carbon peak at top and bottom and are fairly stable in the middle $\delta^{15}N$ and $\delta^{13}C$ are lowest at top and bottom but the $\delta^{13}C$ also reach a low just above the middle. The carbon/nitrogen ratio is fairly stable throughout with one little peak just above the middle. C2 (Fig. 4.12) is 11.7 cm long, unlaminated throughout, and is very dark grey (5Y 3/1) mottled with black (5Y 2/1). There are also a few black streaks in the bottom 2 cm. Coarse sediment is present throughout but peaks in the middle section. Bulk density ranges between 0.4-0.7 g/cm^3 and MS is fairly constant throughout. The mean grain size is around 11 μm and peaks at 8.25 cm. The composition peaks slightly at 8.25 where clay is 41%, silt is 54%, and sand is 5% but in general is about 44%, 54% ,and 2%, respectively. Biogenic silica peaks again at top and bottom of the core and ranges between 2.6 and 7.1% (Fig. 4.13). Nitrogen and carbon content increase at the bottom and at the top $\delta^{15}N$ and $\delta^{13}C$ are lowest at the top and bottom and the carbon/nitrogen ration varies throughout with peaks at top, middle and bottom.

The longest core record, C3 (Fig. 4.14) is 20.8 cm. The top 8.8 cm is dark grey (5Y 3/1),mottled with black (5Y 2/1). There is as black layer between 8.8-9.7 cm, then a light olive grey layer (5Y 6/2) between 9.7-10.9 cm, followed by another black layer between 10.9-11.4 cm. The rest is very dark grey. The core is classified as very faintly laminated in the top 8 cm, then faintly laminated from 8-10 cm and the rest is unlaminated. There are layers of coarse sediment

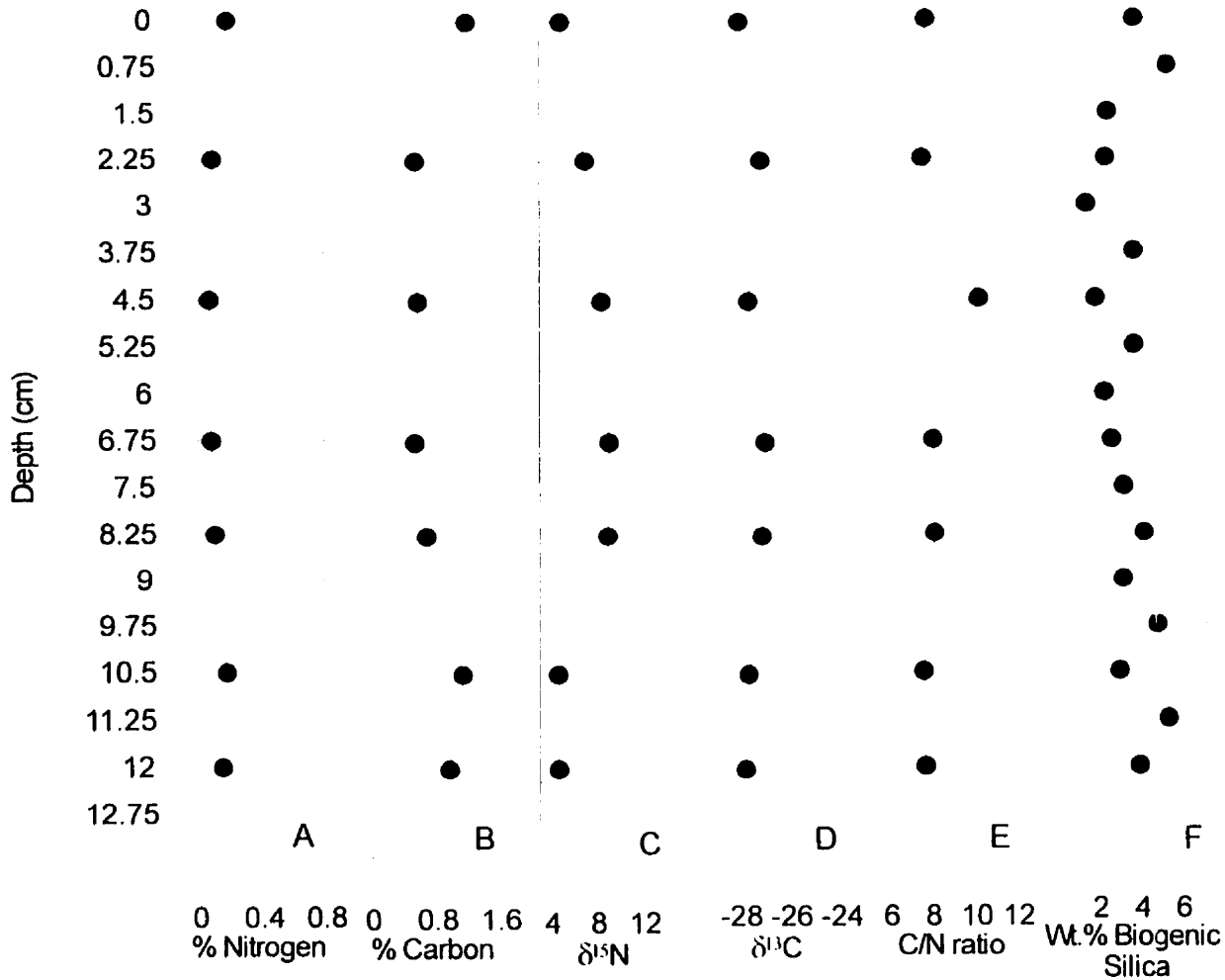

Fig. 4.11 Results of analysis of biogenic properties of the sediment collected in trap B4. (A) % nitrogen, (B) % carbon, (C) $\delta^{15}N$, (D) $\delta^{13}C$, (E) the carbon/nitrogen ratio, and (F) the weight percent biogenic silica.

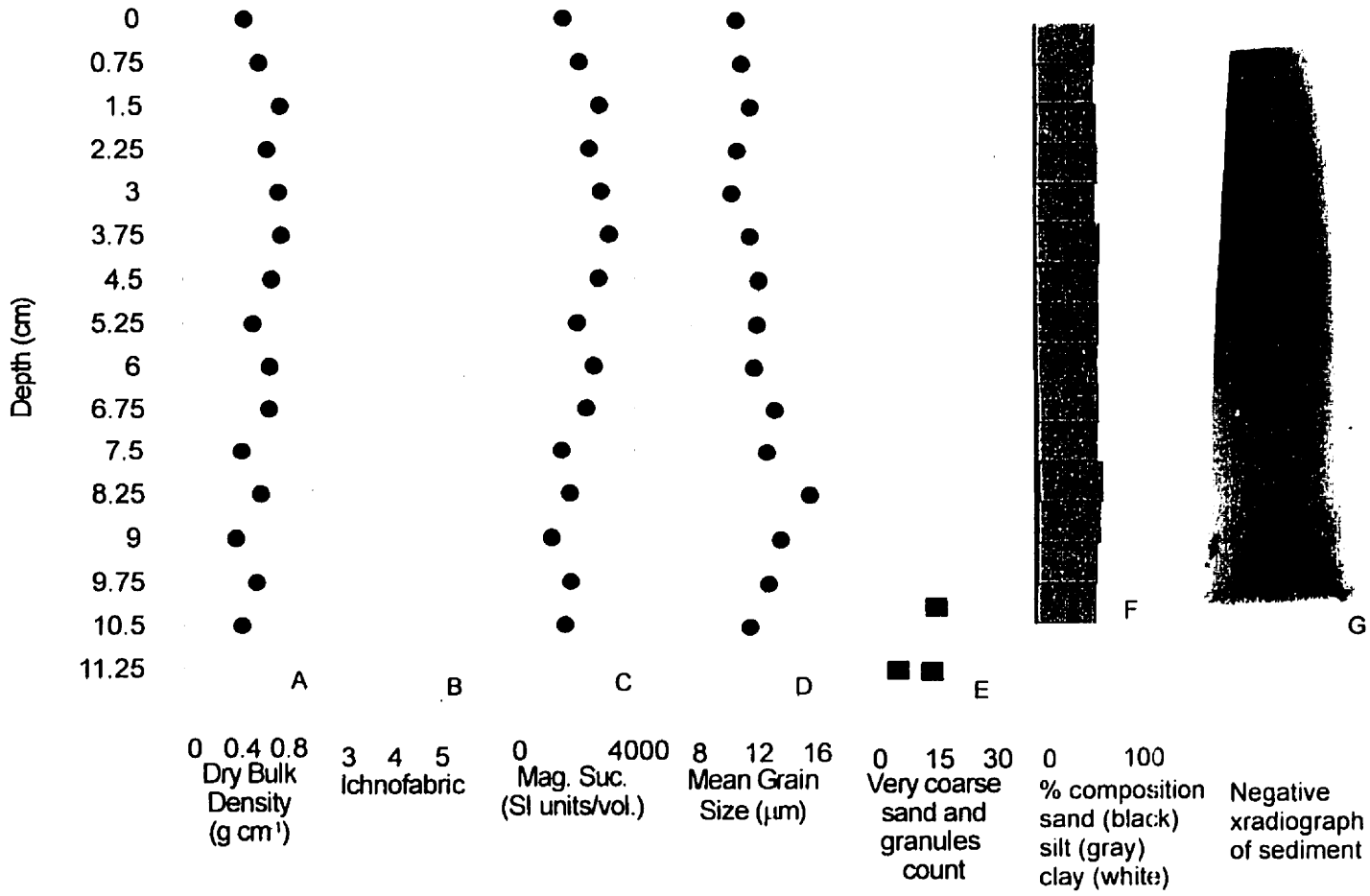

Fig. 4.12 Results of analysis of sediment collected in trap C2.
See Fig. 4.2 for information on each graph.

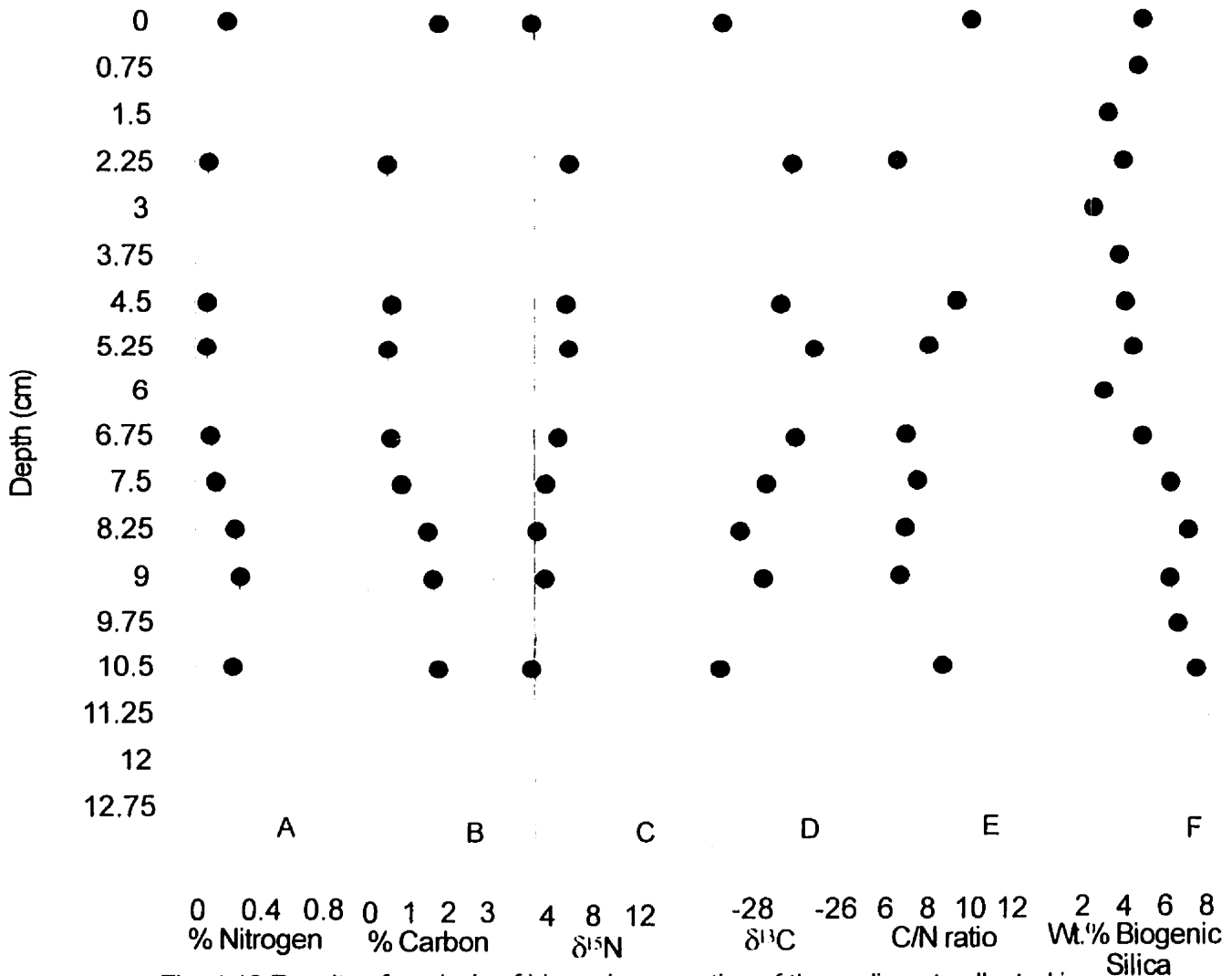

Fig. 4.13 Results of analysis of biogenic properties of the sediment collected in trap C2. (A) % nitrogen, (B) % carbon, (C) $\delta^{15}N$, (D) $\delta^{13}C$, (E) the carbon/nitrogen ratio, and (F) the weight percent biogenic silica.

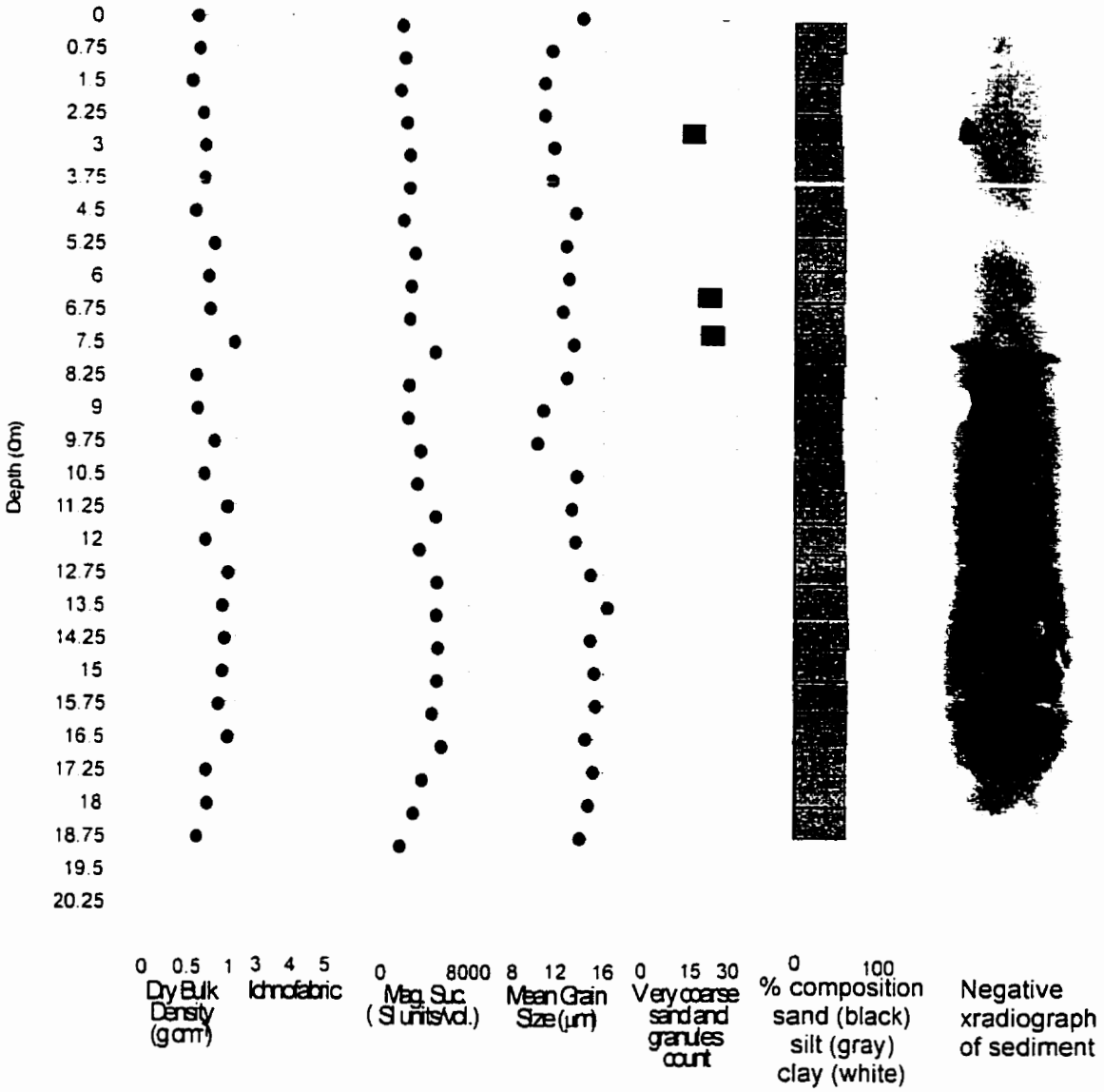

Fig. 4.14 Results of analysis of sediment collected in trap C3. See Fig. 4.2 for information on each graph.

in the top 8 cm and also some in the bottom 2 cm. The bulk density fluctuates between 0.5 and 1 g/cm^3 with the peak at 7.5 cm. The same peak is seen in the MS but there is less fluctuation overall. Mean grain size fluctuates around 12 μm and is lowest in the area of light sediment where there is no sand. The composition down to 13.5 cm is about 44%, 54%, and 2% clay, silt, and sand, respectively. In the bottom this changes to about 40%, 57%, and 3%. The biogenic silica has a high peak of 11% at the top, then ranges between 2.8 and 6.4 % with smaller peaks in the middle (below the light layer) and the bottom. (Fig. 4.15). Nitrogen and carbon peak at the top and bottom and are fairly low throughout. $\delta^{15}N$ and $\delta^{13}C$ reach lowest levels at the bottom and $\delta^{15}N$ also at the top, whereas $\delta^{13}C$ is variable throughout. The carbon/nitrogen ratio varies throughout.

C4 (Fig. 4.16) is 17.2 cm very dark grey (5Y 3/1) and mottled with black (5Y2/1). Most of the core is very faintly laminated but between 10 and 13.5 cm it is faintly laminated. There is coarse material spread fairly evenly throughout the core. Bulk density is between 0.4 and 0.8 g/cm^3 and lowest at the top and bottom, and this pattern is seen in MS as well. Mean grain size is around 11 μm down to 8.25 cm where it increases slightly. The sediment is composed of about 42.5 % clay, 56% silt, and 1.5 % sand in the middle part but about 35%, 62%, and 35% clay, silt, and sand, respectively, in the top and bottom. Biogenic silica peaks at 0.75 cm and 13.5 cm with 6.6 and 7.9% respectively. The lowest value is 2.5% (Fig. 4.17). The nitrogen and carbon content peak at the top and bottom

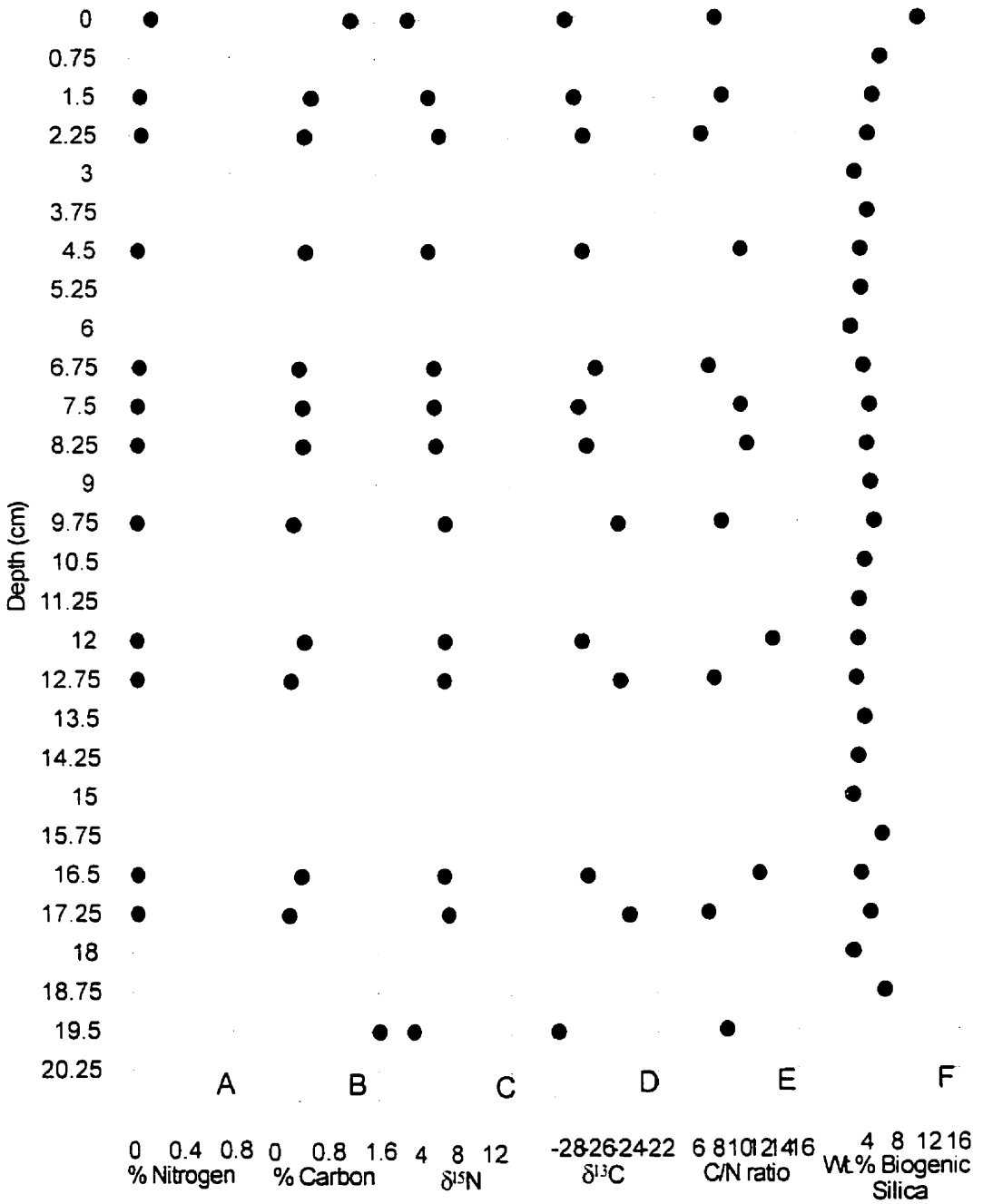

Fig. 4.15 Results of analysis of biogenic properties of the sediment collected in trap C3. (A) %nitrogen, (B) %carbon, (C) ^{15}N, (D) ^{13}C, (E) the carbon/nitrogen ratio, and (F) the weight percent biogenic silica.

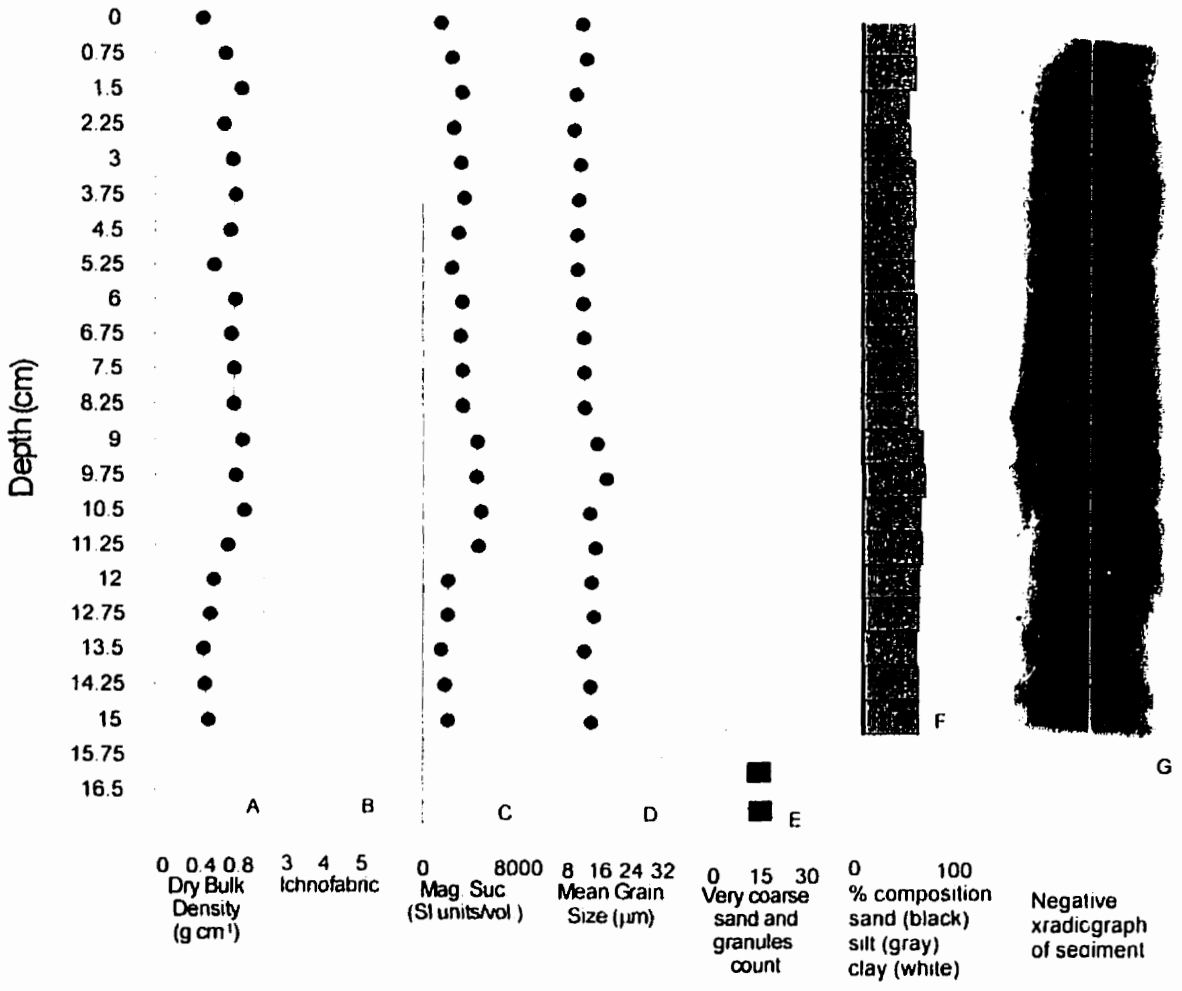

Fig. 4.16 Results of analysis of sediment collected in trap C4.
See Fig. 4.2 for information on each graph

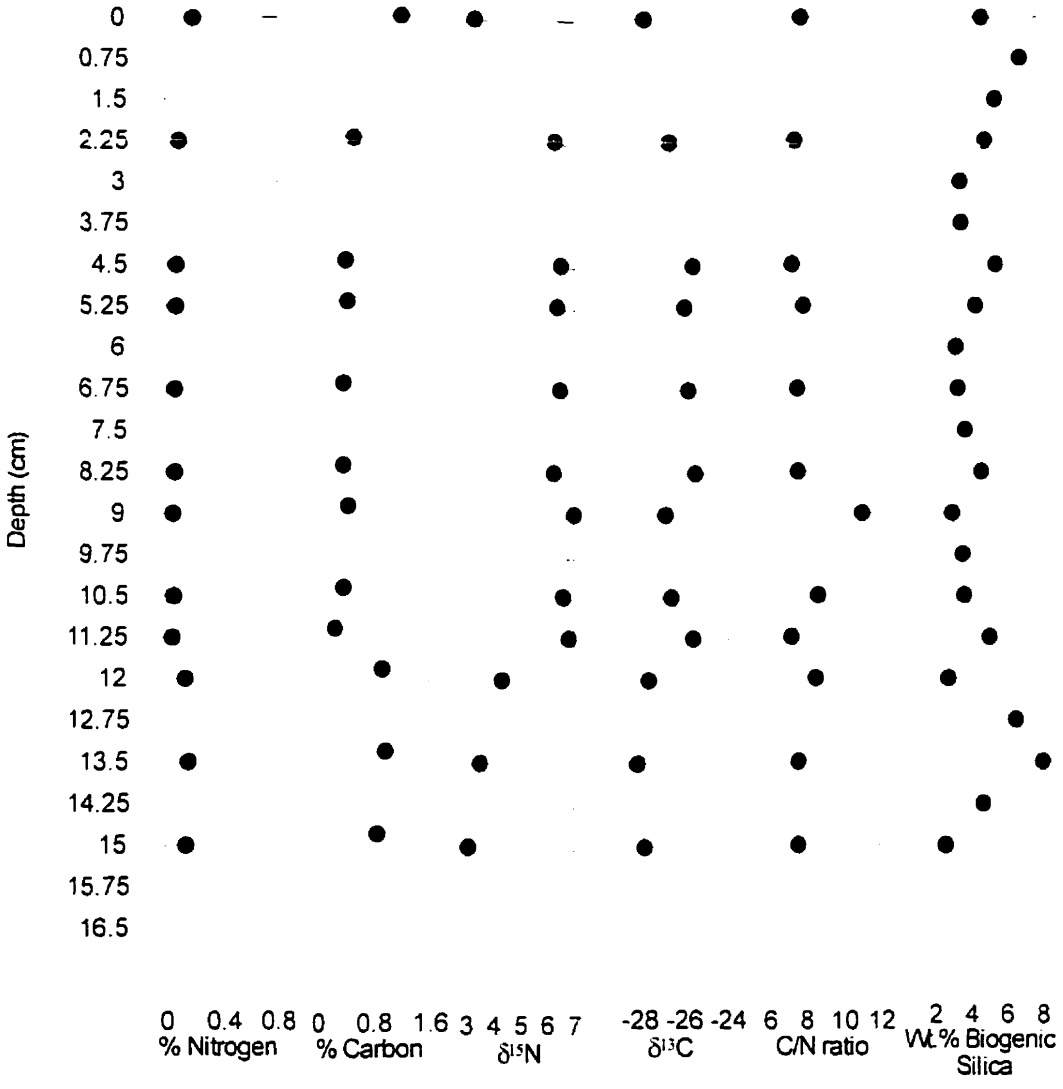

Fig. 4.17 Results of analysis of biogenic properties of the sediment collected in trap C4. (A) nitrogen, (B) carbon, (C) ^{15}N, (D) ^{13}C, (E) the carbon/nitrogen ratio, and (F) the weight percent biogenic silica.

with fairly low values in the middle. $\delta^{15}N$ and $\delta^{13}C$ reach lowest values at the top and bottom and are fairly stable through the middle. The carbon/nitrogen ratio is fairly low and stable throughout but has one peak in the middle.

4.4.2. Spatial Variation

The total sediment flux by weight (Fig. 4.18 a) in each trap increased with depth in moorings A, and B, with more sediment in B than A. In mooring C there was higher flux in the third trap than in the fourth trap. This trap (C3) also had the highest sediment accumulation of all traps retrieved. Yet, when flux was expressed as thickness (mm a^{-1}) there was a smaller difference between the two proximal sites (A and B), and the distal site (C) still had the highest accumulation (Fig. 4.18 b).

Rates of accumulation, and mean values of MS, grain size, and biogenic silica are listed in Table 4.2 to give a spatial comparison between trap sites. The mean grain size is highest in mooring B in both traps but higher in the middle trap than in the bottom trap. Mooring A has the smallest mean grain size and there are no significant changes throughout the water column. Mooring C has slightly larger grain size than mooring A but does not show any large changes throughout the water column either.

The mean sand content by relative volume is highest in mooring B; moorings A and C have similar relative volumes, except in the top trap where mooring C has slightly more. The MS is highest overall in mooring C and lowest in mooring A. There is an increase of almost 60% from trap 2 to trap 3 in mooring C, then it drops (to about 30% of the value in trap 2) below trap 4 in

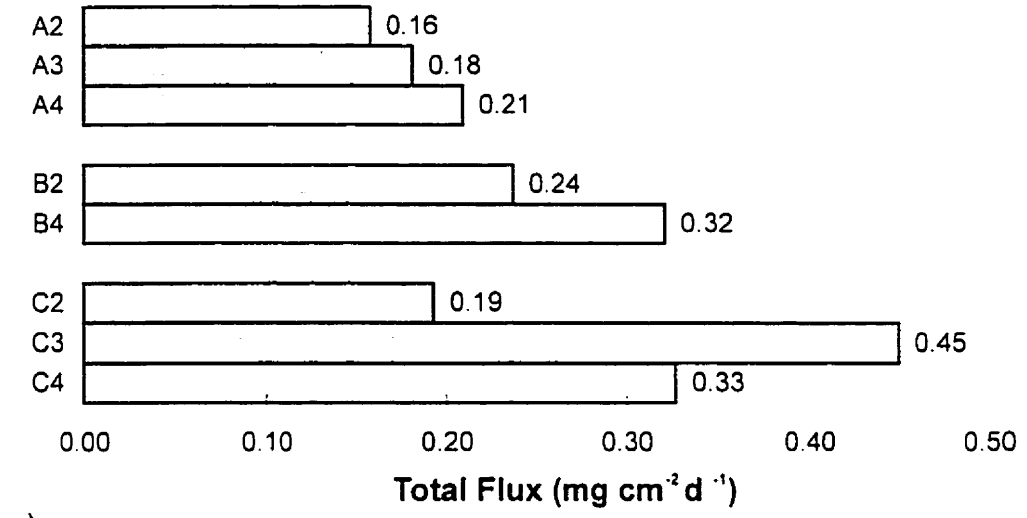

a)

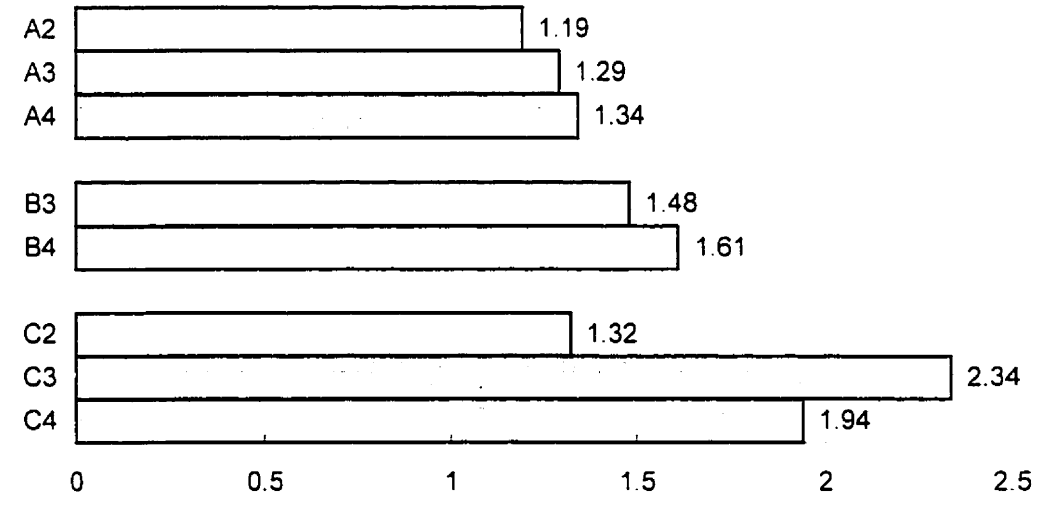

b)

Fig. 4.18
Total flux in each sediment trap. Flux shown as both weight (a) and volume (b). Moorings A and B were ice proximal and mooring C was ice distal.

Table 4.2 Mean values of total flux, magnetic susceptibility, grain size, composition, nitrogen and carbon content, nitrogen and carbon isotopes, carbon and nitrogen ratio, and biogenic silica for each trap.

Trap	Depth m	Rate of accumulation mg m^{-2} d^{-1}	mm a^{-1}	Mag. sucept.	Mean grain size (μm)	Sand vol. %	Silt vol.%	Clay vol.%	%N	%C	$\delta^{13}C$	$\delta^{15}N$	C/N	Bio.silica (wt.%)
A2	386	0.1584	1.19	1976	11.67	2.26	54.15	43.59	0.117	0.662	-26 669	4.692	6.865	4.29
A3	496	0.1818	1.29	2152	11.67	2.22	59.34	38.44	0.100	0.663	-26 866	6.417	7.738	3.86
A4	545	0.2089	1.34	2580	12.32	2.48	54.65	42.87	0.085	0.687	-26 817	5.132	9.143	4.05
B3	565	0.2367	1.48	2683	12.36	4.60	54.83	40.57	0.134	0.963	-27 546	4.567	8.662	4.33
B4	620	0.3209	1.61	3240	13.88	3.32	56.49	40.18	0.120	0.883	-27 502	6.157	8.043	3.38
C2	411	0.1930	1.32	2157	12.10	2.62	53.52	43.86	0.159	1.085	-27 591	4.385	7.984	4.96
C3	565	0.4504	2.32	3798	12.36	2.15	56.52	41.35	0.087	0.594	-26 302	5.809	9.292	4.32
C4	645	0.3269	1.94	3058	12.70	2.40	56.82	40.78	0.090	0.604	-26 600	5.540	7.935	4.96

mooring B at the bottom. The mean biogenic silica weight % in the traps is almost the same in each mooring except in B4 where it is much smaller. Table 4.3 lists the diatom species found in the sediment (Leventer, personal communication).

4.5. Discussion

On return to Lallemand Fjord in April 1999, there was a striking difference in the number and size of icebergs on the surface compared to the conditions in 1998 (Fig. 4.19). Several large tabular icebergs were present near the ice shelf. By measuring the distance from the port and stern of the ship to the ice front, and comparing those points to the position of the ice edge in 1998 (from the acoustic survey), an estimated 200-900 m had broken off the ice shelf. Mean monthly temperatures recorded at Rothera show that the area had experienced a relatively warm period. The mean annual temperature over the past 25 years was -4.7°C but during the study period the mean temperature between the trap deployment and recovery was -2.2°C (Fig. 4.20). The combination of icebergs in front of the ice shelf and the warm temperatures during the study period suggests that the ice shelf is continuing to disintegrate and that this is, at least partially, a response to warmer temperatures.

4.5.1 Sediment flux

The total flux measured in each trap, except C3, (Table 4.2) lies within the 1-2 mm a^{-1} sedimentation rate in Lallemand Fjord that has been estimated from sediment cores (Domack and McClennen, 1996; Stein, 1992). Particles collected in traps are not only those that have a high enough settling velocity to

Table 4.3 List of diatom species found in the sediment traps (Leventer, personal communication).

Achnanthes spp.
Amphora sp.
Chaetoceros spp.
Cocconeis spp.
Corethron criophilum
Eucampia antarctica
Fraglariopsis angulata
Fragilariopsis curta
Fragilariopsis kerguelensis
Fragilariopsis lineata
Fragilariopsis peragallii
Grammatophora spp.
Leptocylindrus sp.
Licmophora spp.
Navicula glacei
Pinnularia quadratarea
Rhizosolenia spp.
Stellarima microtrias
Synedra spp.
Thalassiosira antarctica
Thalassiosira tumida

(sp.= one species observed but not identified to species level; spp.=several species seen within that genus)

A

B

Fig.4.19 Photographs showing the amount of ice present at the Müller Ice Shelf in 1998 (A) and 1999 (B).

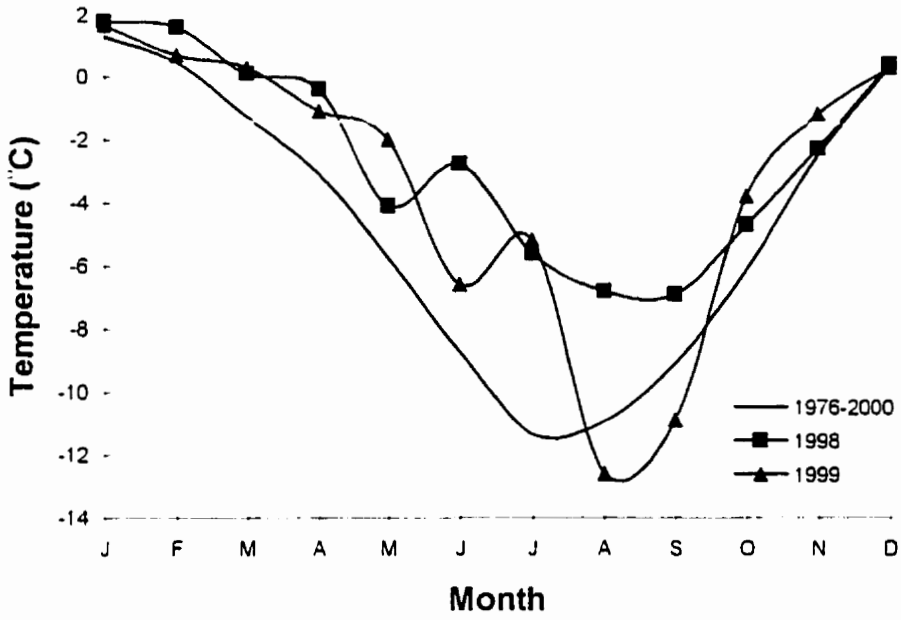

Fig. 4.20 Comparison of mean monthly temperatures at Rothera station between 1976-2000 (until feb.) with the mean monthly air temperatures in 1998 and 1999. Traps were in the water between March 1998 and April 1999.
Data supplied by the British Antarctic Survey, Cambridge, UK.

fall vertically, but also those transported horizontally by currents in the water column. Currents create eddies in the traps which resuspend material that has not yet been able to settle. The circulation pattern of these eddies determines the residence time of a particle in the trap and this is referred to as the trap efficiency (Gardner, 1980).

Trap efficiency for funnel-shaped sediment traps can be improved by the use of baffles. Total flux can only be measured accurately by open funnel traps if the water is still, but the flux will be underestimated if there are currents around the trap (Gardner, 1980). Bloesch and Burns (1980) found the trap efficiency for open funnels to be 25-60 % but that baffles were efficient in reducing the turbulence in traps and increase the efficiency to 60-90 % . Since baffles were used in this study, and the sediment flux agrees with that calculated from cores, it suggests it is a valid estimation of the annual flux.

4.5.2 Spatial variations among moorings

The higher sediment flux in C3 might reflect lateral transport by mid water currents. A silt-sized particle with a density of 2650-2900 kg m^{-3} in water at 0°C falls at a velocity that is less than 5 mm s^{-1} (Gilbert, 1990). Thus, it only takes a weak current to transport sediment laterally. Since the sediment collected in C3 is mainly composed of silt and clay-sized material, it is possible that currents influenced the distribution and deposition of these particles. Mammone (1992) interpreted an increase by a factor of three from the top trap to the bottom trap to show settling from resuspension. The increase in sediment in C3 almost doubles (1.8) from C2 to C3; however, C4 has less sediment than C3. This could be

caused by lateral transport of sediment in mid-water layers, at the level of C3, that reduces the amount of sediment available for deposition at the bottom trap.

Additional spatial variation among the moorings is observed in the grain size data. The traps in mooring B receive more sand than the other moorings. All traps contain well-sorted sand (appendix) but B3 is the only trap where a high influx of well-sorted sand is seen. At the highest influx the sand content is 15%, whereas the sand content in other traps remains below 6%.

4.5.3 Temporal variation within traps

Coarse material occurs uniformly throughout the record at the ice-distal sites, indicating either that there was some deposition of ice-rafted material through the year, or more likely that both rafting and fine-grained deposition from suspension during winter decreased to near zero. This was found in the Weddell Sea where time-series sediment traps were used which measured collected sediment in 24 different known times and over a one year period. The highest flux reached the traps in March but the overall high flux period began in mid January and lasted until the end of April (Honjo, 1990). Dunbar *et al.* (1998) also found the highest sediment fluxes during January and February in the Ross Sea. If this sedimentation pattern can be applied at the MIS then the sediment in the traps mainly represents the open water season in 1998 and 1999.

The peaks in biogenic silica are not as distinct as those seen in other areas, for example the Ross Sea (Dunbar *et al.*, 1998) and the Weddell Sea (Honjo, 1990). The peak in Lallemand Fjord is only about 6% (11% at the highest peak) and the difference from high and low is only about 2-3% on

average. In the Weddell Sea biogenic opal was 79% and in the Ross Sea 83% by weight. However, if sedimentation became very low at the MIS during the winter season, as suggested by the coarse sediment flux, then the biogenic material in the record represents all of that produced during the spring melt and open water season. In that case biogenic silica increased to 11% at the most, but to about 6% on average, during high productivity at the MIS.

Subtle peaks in nitrogen and carbon content, as well as small lows in the carbon and nitrogen isotopes might represent the times of higher production at the site. These highs and lows are present at the top and bottom of most traps. Higher availability of nitrogen and carbon occurs during spring when ice melts and releases nutrients. The corresponding $\delta^{13}C$ decrease implies a greater degree of carbon uptake at the surface and the concordant $\delta^{15}N$ decrease shows greater availability of nitrogen for biogenic production (Sackett, 1989; Faure, 1986; Anderson and Arthur, 1983; Kaplan, 1983). It is interesting to note that the $\delta^{13}C$ measured in the Andvord Bay traps were higher than at the MIS. The three traps had isotope values of -25.609, -22.691, and -24.818 with depth (Domack, personal communication). This suggests that ice conditions sometimes are more severe in Andvord Bay, a sub-polar fjord, than in Lallemand Fjord. However, the $\delta^{13}C$ normally ranges between -24 and -30 for particles collected through a winter season. Significant sea ice conditions can bring the value up to -23 (Dunbar, personal communication).

Diatom species in the trap record could reflect seasonal variation in the ice cover. A low abundance of a few diatom species is present in the traps.

Taylor *et al.* (submitted) found three different diatom assemblages associated with variations in sea ice. Two groups of diatoms were associated with sea ice. One of them reflected loose sea ice and the other more compact multi-year or fast ice. The third group reflected open-water conditions. Some of the diatoms reflecting open-water conditions were *Eucampia antarctica*, *Fragilariopsis kerguelensis*, and *Synedra* sp. Diatoms representing sea ice were genera such as *Navicula*, *Rhizosolenia*, and *Synedra*. All of these diatoms were seen in the trap record (Leventer, personal communication). One of the most common species of diatom was *Thalassiosira antarctica*. This species was part of all three assemblages as was *Fragilariopsis curta*. (Leventer, personal communication). A detailed diatom count might reveal assemblages representing seasonal ice and open water conditions during the study period.

4.5.4 Trap data compared with previous studies

The higher amount of well sorted sand in the proximal site corresponds with core records. Stein (1992) suggests that sand at ice proximal sites reflects an aeolian or meltwater origin and deposition at the ice edge. Fredericks *et al.* (1991) suggested that well-sorted sand with high magnetic susceptibility in proximity to the ice shelf is aeolian sediment eroded from exposed bedrock and composed of heavy magnetic minerals. The well sorted sand influx at B3 has a corresponding peak in magnetic susceptibility. This is evidence that the origin of the sand-rich layers in sediment cores from this site is aeolian transported debris. The sand could either have been deposited over the ice edge or it is

likely that the extensive calving released sediment that had been deposited in crevasses by aeolian processes.

Biological productivity is low in Lallemand Fjord. The amount of biogenic matter in the traps was low compared to the sub-polar fjords in the peninsula. For example, percentages of biogenic silica and organic carbon in Andvord Bay are between 22.6 - 30 % and 3.4 - 4.7%, respectively (Mammone, 1992). It has been suggested that a low amount of biogenic material indicates a higher supply rate of terrigenous matter (Domack and McClennen, 1990). This has been seen in sub-polar settings. However, in this polar setting it is likely that meltwater into the fjord is relatively low and causes the overall supply of terrigenous matter to be low. Domack and Ashley (in prep.) did not see a distinct freshwater layer at the surface adjacent to the MIS, only a slight decrease in salinity. In addition, production of biogenic matter may be reduced due to the lack of fresh water available to stabilise the water column which is necessary for phytoplankton growth. The effect of low meltwater supply at the ice shelf suggests that the low biogenic content in the sediment is caused by lower phytoplankton production.

Several CTD casts made in Lallemand Fjord indicate transport of sediment in mid-water layers. In fjords to the north, mid-water transport has also been observed but in combination with cold water tongues. These features are best developed near glacial termini. In addition, near bottom turbidity has been seen and is also an important part of the sediment transport in these fjords (Domack *et al.*, 1994; Domack and Williams, 1990). Although, the mid-water sediment layers in front of the MIS had an increase in sediment concentration

(Brandon, 1998), they were not associated with cold water tongues. Therefore, it seems the mid-water transport is attributed to the CDW present at the ice shelf and not by the small amount of melt water produced at the ice shelf.

Laminations have been documented in sediment cores from Lallemand Fjord (e.g. Shevenell *et al.*, 1996). Such sediment structures were not found in the sediment traps even though they have been suggested to represent ice-proximal melt events. What looked like very faint laminations in the xradiographs were not detectable in the trap sediment. It is possible the processes producing sedimentary structures might take place at the sea floor. The acoustic survey from 1998 indicates that the sea floor in front of the MIS is irregular and is partially covered with sediment that is about 10 m thick (Gilbert, personal communication). The record also suggests that sediment is thicker in depressions and thinner on rises. There is no other pattern to the thickness and distribution of the sediment cover. The irregularity of the sea floor might cause mass wasting at steep side walls, resulting in laminations.

There was an obvious qualitative difference in the sediment collected in trap C3 compared to all other sediment traps. There was a light coloured layer located at 9 cm depth in C3 which was not observed in any of the other seven sediment traps. The 9 cm layer in C3 was characterised by a small mean grain size and an absence of sand sized particles. Trap C3 differed from all other traps in 3 ways: 1) it had the highest average magnetic susceptibility, 2) the highest sediment flux and, 3) received the highest peak in biogenic silica at the top of the record. However, at the 9 cm level, the amount of biogenic silica and

organic carbon was similar to that observed in the other traps and this layer also turned olive green when exposed to air. The traps above and below trap C3 did not exhibit the distinct light coloured layer. The origin of this layer is not clear.

4.6 Conclusion

Spatial variation among traps suggests that very fine to fine well-sorted sand is deposited in the ice-proximal environment as a result of deposition from aeolian processes. Higher flux at the middle trap of mooring C indicates possible sediment transport in mid-water layers.

Temporal variations within traps suggest possible seasonal layers of productivity and release of clastic sediment at ice melt. Coarse material throughout the record in the distal traps suggests that sediment deposition ceased during the winter season. In that case the biogenic silica represents the diatom production that occurred during the spring melt season. This shows that seasonal productivity at the MIS is much smaller than in the sub-polar fjords in the peninsula.

There is agreement between the trap data and sediment cores. For example, core studies suggest sediment enters the fjord from undermelt of the ice shelf and settles out of suspension in the water column. Well-sorted sand is deposited at the ice edge. Sediment transport in mid-water layers are present near the ice shelf. It is possible that diatom assemblages in the trap samples could indicate what the sea ice conditions were like during the collection period but this has to be concluded with a formal diatom count.

The sediment sources at the MIS are controlled by environmental factors. Undermelt of the ice shelf is dependent on the presence of the warm CDW. Deposition of sand layers at the ice edge depends on the ice shelf position and calving frequency. Since ice shelves appear to be sensitive to temperature changes, temperature would also control the deposition of sand. Coarse sediment at distal sites is deposited at ice break up and by icebergs. A lack of such material would indicate that calving of the ice shelf did not occur and/or that no sediment was released. Productivity of phytoplankton is dependent on a stable water column and is therefore controlled by temperature as the amount of fresh water produced during spring melt controls the stability of the water column. Lastly, diatom assemblages indicate dependence on ice type.

Chapter 5: Summary and future work

5.1 Summary

The recent retreats of several ice shelves, in response to increased temperatures in the Antarctic Peninsula, are different from normal calving in that they are continuous and without any substantial readvance (Vaughan and Doake, 1996). Understanding the significance of these retreats in relation to natural ice shelf variability is important for the understanding of human-induced global change.

This study examined the ice-proximal sedimentation processes at the Müller Ice Shelf (MIS) in Lallemand Fjord, Antarctica. The MIS is of interest because it is situated right at the limit of viability for ice shelves and is currently retreating. In fact, aerial photos and satellite images show that the MIS has reached its minimum recorded extend since the 1940's (Ward, 1995). Continuos calving of the ice shelf took place during the study period and temperature records from the nearest research station indicate that the air temperature was above average during this time.

A knowledge of the modern sedimentary environment at the MIS is needed for an evaluation of how the ice shelf has fluctuated in the past. Previous studies at the MIS suggest that it is possible to track the ice shelf edge by looking at the down-core variability of sand and organic content in the composition of the sediment. It is believed that the sediment from beneath an ice edge will contain fine-grained material that has melted out from the base of

the ice shelf (Domack and Ashley, in prep.; Brandon, 1998). The ice edge sediment should also contain well-sorted sand as a result of deposition from aeolian processes (Domack and Stein, 1993; Stein 1992; Fredericks *et al.*, 1991). Away from the ice edge should be more coarse material in form of ice-rafted debris as a result of deposition from icebergs (Domack *et al.*, 1995).

To check this theory, a study on the modern sedimentary processes at MIS was carried out. It was expected that there would be property differences in the material collected at the ice-proximal sites compared to the ice-distal site. Three moorings with four traps each were used. The traps were positioned at different levels in the water column so that possible sources and transportation processes at different levels could be detected. Sediment was collected in traps during 394 days, then analyzed for spatial and temporal variation. A temporal record could potentialy increase the resolution with which cores can be interpreted.

The sediment sources in Lallemand Fjord today are from meltout, aeolian processes, IRD, and sediment produced at the ice front during spring melt as phytoplankton blooms. Sediment settles through the water column and some is transported in mid-water layers or by rafting. Thus, some sand layers are found at their point of entry at the ice edge, whereas silt-sized particles and fine sand have been transported and accumulated away from the ice front.

These sediment sources are controlled by climate. For example, a reduction in spring melt would reduce the amount of phytoplankton produced at

the surface, and this would affect the biogenic content in the sediment. In addition, reduced melting could also reduce the amount of terrigenous matter brought to the water column. This could be caused either by decreasing air temperatures or a change in the CDW that appears to be important in the undermelt of the ice shelf today. Lower temperatures could also reduce calving and as a result, there would be a decrease in the amount of IRD at distal sites and possibly also reduced sand fluxes at the ice edge.

The sedimentary record collected over 13 months in this study did not show distinct differences between proximal and distal sites. All traps contained well-sorted sand, some ice-rafted debris, and did not show a disitinct difference in organic content. This might indicate that the presence of this ice shelf will be reflected in the sedimentary signal with some distance from its edge. Thus, the precision of determining the position of this ice shelf edge can not be better that within 3.7 km minimum (the distance between the ice edge and the distal mooring site).

5.2 Future work

This study represents one year of deposition at the MIS. It was a year when the mean monthly temperatures were recorded as above average and the sediment is thus representative of warm conditions. Therefore, it would be beneficial to continue the sediment trapping over a few years to compare modern sediment deposition during cold and warm years. However, a few

changes to the methods and mooring design would help in the interpretation of the data.

Firstly, as the sediment traps were designed with only one collection cup each, there are no time markers that can indicate what time periods of the year are represented in the samples. A new study would benefit from traps using rotational cups where the collection period is known. However, the idea with the traps used in this study was to be able to preserve any sedimentary structures. Thus, a way of marking the sediment with a sedimentary marker at certain time intervals would have been useful for the determination of time.

Secondly, current meters at different levels in the water column would strengthen the interpretation of sediment deposition at the MIS. These would help in establishing the nature and positions of mid-water currents in front of the ice shelf as well as in understanding the presence of the CDW and its impact on sediment transport.

Thirdly, by collecting surface sediment during the phytoplankton bloom it would be possible to determine the actual productivity at the surface and how biogenic matter is preserved as it passes through the water column and is deposited on the sea floor.

A detailed study of the diatoms could give an idea of the amount of melt water produced at spring melt and indicate what the sea ice conditions were like during the study period. Finding the ratio of *Fragilariopsis curta* and *F. cylindrus* to *Thalassiosira antarctica* gives an estimation of the volume of low salinity sea

ice melt water that is produced (Leventer *et al.*, 1996). Comparing the entire diatom assemblage with the three groups found to represent ice conditions (Taylor *et al.*, submitted) and periods of open water would contribute to higher resolution of a seasonal interpretation.

References

Aarseth, I., Lønne, Ø., and Giskeødegaard, O. 1989. Submarine slides in glaciomarine sediments in some western Norwegian fjords. *Marine Geology,* **88**, 1-21.

Anderson, T.F., and Arthur, M.A. 1983. Stable isotopes of oxygen and carbon and their application to sedimentologic and paleoenvironmental problems. *In:*Arthur, M.A., Anderson, T. F., Kaplan, I.R., Veizer, J., and Land, L.S. *Stable isotopes in sedimentary geology*, SEPM, Tulsa, OK.

Anderson, J.B., and Ashley, G.M. 1991. Glacial marine sedimentation; Paleoclimatic significance; a discussion. *In:* Anderson, J.B., and Ashley, G.M., (eds.) *Glacial marine sedimentation; Paleoclimatic significance.* Boulder, Colorado, Geological Society of America Special Paper 261, 223-226.

Anderson, J.B., Kurtz, D.D., and Weaver, F.M. 1979. Sedimentation on the Antarctic continental slope. *Society of Economic Paleonotolgists Special Publication,* **27**, 265-283.

Anderson, J.B., and Molnia, B.F. 1989. Glacial-marine sedimentation. *Short course in geology: volume 9*, American Geophysical Union, Washington, D.C.

Barrett, P.J., Pyne, A.R., and Ward, B.L. 1983. Modern sedimentation in McMurdo Sound, Antarctica. *In:* Oliver, R.L., James, P.R., and Jago, J.B. (eds.) *Antarctic earth science*, Canberra, Australian Academy of Science, 550-554.

Blankenship, R.B., Rooney, S.T., and Bentley, C.R. 1989. Sedimentation beneath ice shelves - the view from ice stream B. *Marine Geology,* **85**, 101-120.

Bloesch, J. and Burns, N.M. 1980. A critical review of sediment trap technique. *Schweizier zeitschrift der Hydrologie*, **42**, 15-55.

Boggs, S. Jr. 1995. (2nd ed.) *Principles of sedimentology and stratigraphy.* Prentice Hall Inc., Englewood Cliffs, NJ.

Brandon, J. 1998. *The relationship between warm Circumpolar Deep Water and the composition and distribution of suspended particulate matter within Lallemand Fjord, Antarctica.* BA thesis, Hamilton College, Clinton, NY.

Church, M. 1972. Baffin Island sandurs: A study of Arctic fluvial processes. *Geological survey of Canada bulletin*, **216**.

Cowan, E.A., and Powell, R.D. 1990. Suspended sediment transport and deposition of cyclically interlaminated sediment in a temperate glacial fjord, Alaska, USA. *In:* Dowdeswell, J.A. and Scourse, J.D. (eds.) *Glacimarine environments: Processes and sediments.* Geological Society of America, Special publication, **53**, 75-89.

de la Mare, W.K. 1997. Abrupt mid-twentieth-century decline in Antarctic sea-ice extent from whaling records. *Nature*, **389**, 57-59.

DeMaster, D.J. 1981. The supply and accumulation of silica in the marine environment. *Geochim. Cosmochim. Acta*, **45**, 1715-1732.

Doake, C.S.M., and Vaughan, D.G. 1991. Rapid disintegration of the Wordie Ice Shelf in response to atmospheric warming. *Nature*, **350**,

Domack, E.W. 1990. Laminated terrigenous sediments from the Antarctic Peninsula: the role of subglacial and marine processes. *In:* Dowdeswell, J.A. and Scourse, J.D. (eds.) *Glacimarine environments: Processes and sediments.* Geological society of America, Special publication, **53**, 91-103.

Domack, E.W., and Anderson, J.B. 1983. Marine geology of the George V continental ice margin: combined results of deep freeze 79 and the 1911-14 Australian expedition. *In:* Oliver, J. and Jago (eds.) *Antarctic earth science.* Australian Academy of Science, Canberra.

Domack, E., and Ashley, G. in preparation. Glacial meltwater regimes of the Antarctic Peninsula.

Domack, E.W., and Ishman, S. 1993. Oceanographic controls on modern sedimentation within Antarctic fjords. *Geological society of America Bulletin*, **105**, 1175-1189.

Domack, E.W., and McClennen, C.E. 1996. Accumulation of glacial marine sediments in fjords of the Antarctic Peninsula and their use as late Holocene paleoenvironmental indicators. *Antarctic Research Series*, **70**, 135-154.

Domack, E.W., and Stein, A.S. 1993. Late Holocene fluctuations in front of the Müller Ice Shelf, Antarctic Peninsula. *Antarctic Journal of the United States*, **28**, 96-97.

Domack, E.W., and Williams, C.R. 1990. Fine structure and suspended sediment transport in three Antarctic fjords. *Antarctic Research Series*, **50**, 71-89.

Domack, E.W., Anderson, J.B., and Kurtz, D.D. 1980. Clast shape as an indicator of transport and depositional mechanisms in glacial marine sediments: George V continental shelf, Antarctica. *Journal of Sedimentary Petrology*, **50**, 813-820.

Domack, E.W., Foss, D.J.P., Syvitski, J.P.M., and McClennen, C.E. 1994. Transport of suspended particulate matter in an Antarctic fjord. *Marine Geology*, **121**, 161-170.

Domack, E.W., Ishman, S.E., Stein, A.B., McClennen, C.E., and Jull, A.J.T. 1995. Late Holocene advance of the Müller Ice Shelf, Antarctic Peninsula; sedimentological, geochemical, and paleontological evidence. *Antarctic Science*, **7**, 159-170.

Dowdeswell, J. 1987. Processes of glacimarine sedimentation. *Progress in Physical Geography*, **11**, p. 52-90.

Dowdeswell, J.A. and Dowdeswell, E.K. 1989. Debris in icebergs and rates of glacimarine sedimentation: observations from Spitsbergen and a simple model. *Journal of Geology*, **97**, 221-231.

Dowdeswell, J. A. and Murray, T. 1990. Modelling rates of sedimentation from icebergs. *In:* Dowdeswell, J.A. and Scourse, J.D. (eds.) *Glacimarine environments: Processes and sediments.* Geological Society of America, Special Publication, **53**, 105-120.

Dowdeswell, J.A., Villinger, H., Whittington, R.J., and Marienfeld, P. 1993. Iceberg scouring in Scorsby Sund and on the East Greenland continental shelf. *Marine Geology*, **111**, 37-53.

Dowdeswell, J.A., Whittington, R.J., and Marienfeld, P. 1994. The origin of massive diamicton facies by iceberg rafting and scouring, Scoresby Sund, East Greenland. *Sedimentology*, **41**, 21-35.

Dunbar, R.B., Anderson, J.B., and Domack, E.W. 1985. Oceanographic influences on sedimentation along the Antarctic continental shelf. *Antarctic Research Series*, **43**, 291-311.

Dunbar, R. B., Leventer, A.R. and Mucciarone, D.A. 1998. Water column sediment fluxes in the Ross Sea, Antarctica: Atmospheric and sea ice forcing. *Journal of Geophysical Research*, **1093**, 30741-30760.

Dunbar, R.B., Leventer, A.R., Stockton, W.L. 1989. Biogenic sedimentation in McMurdo Sound, Antarctica. *Marine Geology*, **85**, 155-179.

Drewry, D. 1986. *Glacial geologic processes.* Edward Arnold Ltd., London.

Drewry, D.J. and Cooper, A.P.R. 1981. Processes and models of Antarctic glaciomarine sedimentation. *Annals of Glaciology*, **2**, 117-122.

Droser, M.L. and Bottjer, D.J. 1986. A semiquantitative field classification of ichnofabric. *Journal of Sedimentary Petrology*, **56**, 558-559.

Emsile, S.D., Fraser, W., Smith, R., and Walker, W. 1998. Abandoned penguin colonies and environmental change in the Palmer Station area, Anvers Island, Antarctic Peninsula. *Antarctic Science*, **10**, 257-268.

Faure, G. 1986. *Principles of isotope geology. John Wiley & Sons, New York.*

Frederick, B.C., Domack, E.G., McClennen, C.E. 1991. Magnetic susceptibility measurements in antarctic glacial-marine sediment from in front of the Müller Ice Shelf, Lallemand Fjord. *Antarctic Journal of the United States*, **26**, 126-128.

Gardner, W.D. 1980. Sediment trap dynamics and calibration: a laboratory evaluation. *Journal of Marine Research*, **38**, 18-39.

Gilbert, R. 1983. Sedimentary processes of Canadian arctic fiords. *Sedimentary Geology*, **36**, 147-175.

Gilbert, R. 1990. Rafting in glacimarine environments. *In:* Dowdeswell, J.A. and Scourse, J.D. (eds.) *Glacimarine environments: Processes and sediments*. Geological society of America, Special publication, **53**, 105-120.

Gilbert, R. 2000. Environmental assessment from the sedimentary record of high-latitude fiords. *Geomorphology*, **32**, 295-314.

Gilbert, R., Nielsen, N., Desloges, J.R., and Rasch, M. 1998. Contrasting glacimarine sedimentary environments of two arctic fiords on Disko, West Greenland. *Marine Geology*, **147**, 63-83.

Griffith, T., and Anderson, J.B. 1989. Climatic control of sedimentation in bay sand and fjords of the northern Antarctic peninsula. *Marine Geology*, **85**, 181-204.

Grobe, H. 1987. A simple method of the determination of ice-rafted debris in sediment cores. *Polarforschung, 57*, 123-126.

Honjo, S. 1990. Particle fluxes and modern sedimentation in the polar oceans (Ch. 13). *In:* Smith W.O.Jr. (ed.) *Polar oceanography, Part B: Chemistry. biology, and geology.* Academic Press Inc., San Diego, California.

Hulbe, C.L. 1997. Recent changes to Antarctic Peninsula ice shelves: What lesson have we learned? *naturalScience*, **1**, 1-6.

Jacobs, A., Gordon, A.I., and Ardai, J.L. 1979. Circulation and melting beneath the Ross Ice Shelf. *Science,* **203**, 439-443.

Jenkins, A., Vaughan, D.G, Jacobs, S.S., Hellmer, H.H., and Keys, J.R. 1997. Glaciological and oceanographic evidence of high melt rates beneath Pine Island Glacier, West Antarctica. *Journal of Glaciology,* **43**, 114-121.

Kaplan, I.R. 1983. Stable isotopes of sulfur, nitrogen and deuterium in recent marine environments. *In:* Arthur, M.A., Anderson, T. F., Kaplan, I.R., Veizer, J., and Land, L.S. *Stable isotopes in sedimentary geology*, SEPM, Tulsa,OK, 2:1-108.

King, J.C., and Turner, J. 1997. *Antarctic meteorology and climatology.* Cambridge University press, Cambridge, UK.

Krausse, G.L., Schelske, C.L., and Davis, C.O. 1983. Comparison of the wet-alkaline methods of digestion of biogenic silica in water. *Freshwater Biology,* **13**, 73-81.

Lamoureux, S.F. 1994. Embedding unfrozen lake sediment for thin section preparation. *Journal of Paleolimnology* **10,** 141-146.

Leventer, A., and Stevens, L. 1996. Analysis of laminated Antarctic marine sediments. *Antarctic journal - review.* 94-96.

Leventer, A., Domack, E., Ishman, S., Brachfeld, S., McClennen, C., and Manley, P. 1996. Productivity cycles of 200-300 years in the Antarctic Peninsula region: Understanding linkages among the sun, atmosphere, oceans, sea ice, and biota. *Geological Society of America*, **108**, 1626-1644.

Mackiewicz, N.E., Powell, R.D., Carlson, P.R., and Molnia, B.F. 1984. Interlaminated ice-proximal glacimarine sediments in Muir Inlet, Alaska. *Marine Geology,* **57**, 113-147.

Mammone, K.A. 1992. *Modern particle flux and productivity an Andvord Bay, Antarctica.* BA thesis, Hamilton College, Clinton, NY.

Marienfeld, P. 1992. Recent sedimentary processes in Scoresby Sund, East Greenland. *Boreas,* **21**, 169-186.

McKenna Neuman, C. 1993. A review of aeolian transport processes in cold environments. *Progress in Physical Geography,* **17**, 137-155.

Nicholls, K.W. 1997. Predicted reduction in basal melt rates of an Antarctic ice shelf in a warmer climate. *Nature*, **388**, 460-462.

Powell R., and Domack, E., 1995. Modern glaciomarine environments. In: Menzies, J. (ed.) *Modern glacial environments-processes, dynamics, and sediments.* Butterworth-Heinemann Ltd., Oxford, 445-486.

Reynolds, J.M. 1981. The distribution of mean annual temperatures in the Antarctic Peninsula. *British Antarctic Survey Bulletin,* **54**, 123-133.

Ridley, J. 1993. Surface melting on Antarctic Peninsula ice shelves by passive microwave sensors. *Geophysical Research Letters*, **20**, 2639-2642.

Ross, J. D. 1998. *Erosion in the Phewa Tal watershed, middle mountain region, Nepal.* Master's thesis, Queen's University, Kingston, ON.

Sackett, W.M. 1989. Stable isotope studies on organic matter in the marine environment. *In:* Fritz, P. and Fontes, J.C. (eds.)*Handbook of environmental isotopes geochemistry; the marine environment A.* Elsevier, New York, 139-169.

Shevenell, A., Domack, E., and Kernan, G. 1996. Record of Holocene paleoclimate change along the Antarctic Peninsula: evidence from glacial marine sediments, Lallemand Fjord. *Papers and Proceedings of the Royal Society of Tasmania,* **130**, 55-64.

Skvarca, P. 1993. Fast recession of the northern Larsen Ice Shelf monitored by space images. *Annals of Glaciology,* **17**, 317-322.

Smith, N.D. and Ashley, G.M. 1996. A study of brash ice in the proximal marine zone of a sub-polar tidewater glacier. *Marine Geology,* **133**, 75-87.

Smith, W.O. Jr. and Saukshaug, E. 1990. Polar phytoplankton (Ch. 9). *In:* Smith W.O.Jr. (ed.) *Polar oceanography, Part B: Chemistry, biology, and geology.* Academic Press Inc., San Diego, California.

Smith, R.D, Ainley, D., Baker, K., Domack, E., Emslie, S., Fraser, B., Kennettt, J., Leventer, A., Mosley-Thompson, E., Stammerjohn, S., and Vernet, M. 1999. Marine ecosystem sensitivity to climate change; Historical observations and paleoecological records reveal ecological transitions in the Antarctic Peninsula region. *BioScience*, **49**, 393-404.

Stein, A.B. 1992. Growth of the Müller Ice Shelf during the latter half of the Little Ice Age. as documented by glacial marine sediment and radiogeochemistry. B.A. Thesis, Hamilton College, Clinton, N.Y.

Syvitski, J.P.M. 1989. On the deposition of sediment within glacier-influenced fiords: oceanographic controls. *Marine Geology*, **85**, 301-329.

Syvitski, J.P.M. 1991. The changing microfabric of suspended particulate matter-the fluvial to marine transition: flocculation, agglomeration, and pelletization. *In:* Bennet, R.H., Bryant, W.R., and Hulbert, M.H. (eds.) *Microstructure of fine-grained sediments*. Springer-Verlag, New York, 131-137.

Syvitski, J.P.M. and Shaw, J. 1995. Sedimentology and geomorphology of fjords. *In:* Perillo, G.M.E. (ed.) *Geomorphology and sedimentology of estuaries*. Developments in sedimentology, **53**, Elsevier science B.V. 113-178.

Syvitski, J.P.M., Andrews, J.T., and Dowdeswell, J.A. 1996. Sediment deposition in an iceberg-dominated glacimarine environment, East Greenland: basin fill implications. *Global Planetary Change*, **12**, 251-270.

Taylor, F., Whitehead, J., and Domack, E. submitted. Holocene paleoclimate in the Antarctic Peninsula: evidence from the diatom, sedimentary and geochemical record. *Marine Micropaleontology*.

Vaughan, D.G., and Doake, C.S.M. 1996. Recent atmospheric warming and retreat of ice shelves on the Antarctic Peninsula. *Nature*, **379**, 328-331.

Verardo, D.J., Froelish, P.N., and McIntyre, A. 1990. Determination of organic carbon and nitrogen in marine sediment using the Carlo Erba NA-1500 analyzer. *Deep Sea Research*, **37**, 157-165.

Ward, C. 1995. Short note - Mapping ice front changes of Müller Ice Shelf, Antarctic Peninsula. *Antarctic Science*, **7**, 197-198.

Appendix

Physical and biogenic properties of trap sediment

Trap A2

Depth-A2	Bulk densit	Mag Sus	Mean GS	%N	%C	del N	del C	C/N	BSi wt%
0 00	0.59	1998.07	10.83	0.09	0.71	4.48	-28.23	8.85	3.82
0.75	0.72	2859.51	10.26						4.44
1.50	0.61	2340.85	9.96						4.58
2.25	0.56	2092.33	9.88	0.07	0.40	5.91	-26.19	6.85	3.96
3.00	0.53	1857.23	9.58	0.06	0.39	5.57	-26.01	7 09	3.22
3.75	0.49	1890.27	10.39						3.70
4.50	0.50	1930.92	9.52	0.06	0.35	6.11	-25.82	6.70	3.52
5.25	0.70	2670.01	10.36	0.06	0.37	5.42	-25.78	7.15	4.28
6.00	0.56	2060.18	10.07						3.36
6.75	0.49	1951.74	11.22	0.07	0.41	5.07	-26.01	7 25	2.89
7.50	0.46	1808.57	11.21						3.54
8.25	0.43	1512.70	12.52	0.12	0.66	3.97	-26.83	6.49	5.89
9.00	0.46	1759.11	11.64						4 67
9.75	0.44	1615.34	16.89	0.19	1 00	3.52	-27 09	6.04	5.39
10.50	0.53	1734.28	15.59	0.18	0.92	3.75	-27.20	6.11	5.05
11.25	0.50	1535.34	16.80	0.27	1.42	3.13	-27.51	6.13	4.74
11.75									5.52

Trap A3

Depth-A3	Bulk densit	MagSus	Mean grain	%N	%C	del N	del C	C/N	BSi % wt
0.00	0.48	2112.84	12.89	0.10	2.45	4.20	-29 54	27 98	2.63
0.75	0.47	1864.58	11.35						4 71
1.50	0.40	1512.44	11.34	0.12	0.96	4.26	-28.07	9.49	4.02
2.25	0.53	2109.93	11.11	0.10	0.85	5.06	-27 87	9.85	4 58
3.00	0.50	1985.03	11.62	0.07	0.39	6.57	-26.52	6.61	2.48
3.75	0.68	2639.80	11.15						3 15
4.50	0.68	2759.13	11.70	0.07	0.39	7.70	-25.65	6.52	3.38
5.25	0.44	1739.70	10.64	0.10	0.70	7 83	-27.22	8.24	3.97
6.00	0.67	2693.79	11.05						2.46
6.75	0.66	2524 42	11 15	0.08	0.51	7.54	-26.69	7 83	3 26
7.50	0.64	2514.36	11.81						4 26
8.25	0.37	1538.41	10.41	0.08	0.53	7.40	-26.53	7 55	3 64
9.00	0.73	2690.50	14.06						3.68
9.75	0.51	1908.37	11.57	0.08	0.58	7.61	-26.56	8.20	4.55
10.50	0.54	1963.15	11.19						4.53
11.25	0.60	2254.72	12.53	0.11	0.60	6.12	-26.37	6.60	4.56
12.00	0 55	1783.66	12.90						5.83
12.25				0 20	1.12	4.10	-27.18	6.49	

Trap A4

Depth-A4	Bulk densit	MAG SUS	Mean grain	%N	%C	del N	del C	C/N	BSi wt%
0.00	0.47	2037.40	12.68	0.07	0.66	5.04	-27.60	10.97	3.60
0.75	0.83	3649.06	10.67						5.71
1.50	0.83	3841.35	12.56						2.85
2.25	0.58	2586.84	10.86	0.06	0.44	5.85	-26.15	8.81	3.80
3.00	0.82	3753.46	11.95						3.17
3.75	0.73	3279.42	10.59	0.06	0.41	5.86	-26.22	8.33	3.71
4.50	0.57	2343.20	12.79	0.05	0.45	5.23	-26.66	9.71	4.03
5.25	0.56	2375.67	11.26						4.67
6.00	0.46	2083.91	13.90						2.57
6.75	0.53	2079.91	11.26	0.06	0.42	5.41	-26.19	8.35	4.24
7.50	0.70	2950.91	14.46						3.69
8.25	0.81	3305.70	11.89	0.07	0.43	5.18	-25.86	7.05	4.48
9.00	0.44	1740.39	12.67						2.32
9.75	0.66	2565.02	11.16						4.75
10.50	0.46	1666.87	13.17	0.14	1.07	3.85	-27.74	9.16	6.40
11.25	0.57	1949.31	11.82						5.26
12.00	0.46	1658.41	15.79	0.17	1.61	4.65	-28.13	10.75	3.58

Trap B3

Depth-B3	Bulk densit	MAG SUS	Mean grain	%N	%C	del N	del C	C/N	BSi wt%
0.00	0.50	2072.30	17.73	0.19	1.18	2.69	-27.96	7.06	6.34
0.75	0.64	3940.85	22.75						4.17
1.50	0.90	6689.19	30.50	0.05	0.39	5.04	-27.78	8.75	3.07
2.25	0.52	2032.75	12.37	0.09	0.60	5.24	-26.94	7.52	5.02
3.00	0.80	3142.89	13.67						2.84
3.75	0.74	3002.78	10.53						4.55
4.50	0.74	3084.83	12.78	0.10	1.37	6.00	-28.53	15.55	3.24
5.25	0.75	2956.61	11.22						3.80
6.00	0.88	3496.95	11.69						2.58
6.75	0.72	2765.73	12.32	0.07	0.48	6.20	-26.50	7.52	4.31
7.50	0.86	3307.74	13.15						3.92
8.25	0.46	1543.30	12.81	0.11	0.65	4.95	-26.73	6.63	5.69
9.00	0.47	1572.71	12.08						2.49
9.75	0.42	1455.40	14.93						7.34
10.50	0.43	1289.89	16.74	0.23	1.31	3.99	-27.48	6.52	5.94
11.25	0.54	1739.04	14.58						6.64
12.00	0.44	1521.32	16.40	0.21	1.73	2.42	-28.45	9.75	3.92

Trap B4

Depth-B4	Bulk densit	MAG SUS	Mean grain	%N	%C	del N	del C	C/N	BSi wt%
0.00	0.56	2231.25	14.85	0.18	1.21	4.86	-27.95	7.72	3.66
0.75	0.63	2497.96	14.04						5.25
1.50	0.78	3468.06	11.31						2.40
2.25	0.80	3648.39	11.40	0.09	0.55	6.98	-27.10	7.51	2.29
3.00	0.80	5049.00	18.77						1.37
3.75	0.83	4959.61	17.77						3.62
4.50	1.36	3840.01	13.95	0.07	0.59	8.40	-27.60	10.22	1.80
5.25	0.86	3924.67	13.92						3.64
6.00	0.80	3378.33	13.29						2.24
6.75	0.96	4003.80	12.78	0.08	0.55	9.07	-26.93	8.03	2.57
7.50	0.76	2947.61	12.55						3.13
8.25	0.55	2158.00	11.51	0.10	0.69	8.91	-27.07	8.09	4.11
9.00	0.73	2601.53	11.03						3.11
9.75	0.87	3151.04	11.23						4.76
10.50	0.71	2402.80	15.07	0.18	1.15	4.59	-27.60	7.58	2.95
11.25	0.69	2311.16	18.33						5.31
12.00	0.72	2508.44	14.21	0.15	0.98	4.61	-27.73	7.67	3.91
12.75									4.78

Trap C2

Depth-C2	Bulk densit	MAG SUS	Mean grain	%N	%C	del N	del C	C/N	BSi% wt.
0.00	0.44	1561.56	10.66	0.21	1.81	2.78	-28.62	10.24	5.00
0.75	0.57	2114.43	11.01						4.77
1.50	0.75	2801.68	11.59						3.32
2.25	0.64	2448.54	10.70	0.09	0.49	6.08	-26.95	6.66	4.05
3.00	0.74	2847.40	10.32						2.61
3.75	0.76	3125.08	11.57						3.86
4.50	0.67	2765.97	12.17	0.07	0.60	5.76	-27.24	9.51	4.14
5.25	0.51	2026.26	12.06	0.07	0.50	5.99	-26.44	8.16	4.52
6.00	0.66	2599.09	11.86						3.11
6.75	0.65	2326.61	13.25	0.10	0.59	5.10	-26.88	7.09	4.98
7.50	0.41	1473.89	12.70	0.13	0.85	3.97	-27.59	7.62	6.34
8.25	0.58	1758.57	15.64	0.25	1.51	3.20	-28.22	7.02	7.19
9.00	0.36	1128.86	13.64	0.28	1.64	3.88	-27.67	6.76	6.28
9.75	0.54	1790.44	12.83						6.67
10.50	0.42	1591.27	11.55	0.24	1.78	2.70	-28.71	8.80	7.56

Trap C3

Depth-C3	Bulk densit	MAG SUS	Mean grain	%N	%C	del N	del C	C/N	BSi wt%
0.00	0 61	2320.69	13.27	0.18	1.22	3.02	-27 80	8 05	11.31
0.75	0.63	2550.17	10.45						6 30
1 50	0.54	2146.95	9.78	0.08	0.63	5.28	-27 22	8.73	5.25
2.25	0.67	2724.02	9.78	0 09	0.53	6.45	-26.63	6.67	4 60
3.00	0.70	3020.16	10.62						2.84
3.75	0.69	3000.17	10.47						4.50
4.50	0.59	2446.53	12.63	0.06	0.54	5.21	-26.72	10.48	3.54
5.25	0.81	3539.90	11.77						3.63
6.00	0.75	3182.63	12.04						2.26
6.75	0.76	3052.45	11.47	0.07	0.43	5.80	-25.87	7 33	3.88
7 50	1 05	5426.22	12.51	0.05	0.48	5.81	-27.02	10.44	4.66
8.25	0.60	3017.29	11.87	0.05	0.48	5.97	-26.48	11.07	4.30
9.00	0.62	2930.47	9.73						4 78
9.75	0.82	4095.75	9.20	0.05	0.33	6.97	-24.39	8 52	5 23
10.50	0.70	3794.66	12.80						3.96
11.25	0.97	5510.03	12.37						3.22
12.00	0.71	3997.42	12.70	0.04	0 50	6.90	-26.84	13 53	3 08
12.75	0.98	5630.75	14.10	0.04	0.29	6.80	-24.27	7 74	2.82
13.50	0.91	5570 64	15.67						3.90
14.25	0.94	5717.23	14.07						3.05
15.00	0.91	5631.83	14.45						2.35
15.75	0.87	5195.51	14 57						6 15
16.50	0.98	6080.91	13.65	0.04	0.44	6.73	-26 49	12 18	3.39
17.25	0.73	4278.07	14.38	0.04	0 25	7 23	-23.72	7 14	4.60
18.00	0.74	3483.40	13.92						2.35
18.75	0.62	2263.48	13.16	0.21	1.62	3.33	-28 47	8 92	6.47

Trap C4

Depth-C4	Bulk densit	MAG SUS	Mean grain	%N	%C	del N	del C	C/N	BSi wt%
0.00	0.43	1544.66	11.80	0.19	1.23	3.36	-27.72	7.68	4.51
0.75	0.67	2461.15	12.79						6 66
1 50	0.84	3346.60	10.17						5.27
2.25	0.66	2634.59	9.70	0.09	0.54	6.28	-26 62	7 33	4.68
3.00	0.75	3240.62	11.26						3.33
3.75	0.78	3528.31	10.86						3.37
4.50	0.72	3019.13	10.33	0.07	0.41	6.49	-25.57	7.16	5.29
5.25	0.55	2452.79	10.48	0.07	0.44	6.36	-25.94	7.79	4.17
6.00	0.77	3341.29	11.90						3.06
6.75	0.73	3216.59	12.18	0.06	0.38	6.46	-25.76	7 45	3.18
7.50	0.76	3376.87	12.25						3.58
8.25	0.76	3412.76	12.36	0.06	0.38	6 23	-25.45	7 48	4.48
9.00	0.85	4659.52	15.53	0.05	0.45	6.99	-26.79	10.99	2.87
9.75	0.78	4550.34	17.82						3.45
10.50	0.87	4944.53	13.63	0.05	0.38	6.58	-26.54	8.61	3.54
11.25	0.69	4700.15	14.95	0.04	0.26	6.80	-25.53	7.16	4.99
12.00	0.54	2129.19	14.05	0.13	0.94	4.31	-27.55	8.48	2.68
12.75	0.51	2088.05	14.62						6.47
13.50	0.44	1567.70	12.28	0.15	0.98	3.52	-28.03	7.54	7.98
14.25	0.45	1882.59	13.80						4.64
15.00	0.49	2133.65	13.99	0.13	0.87	3.09	-27.71	7.54	2.56

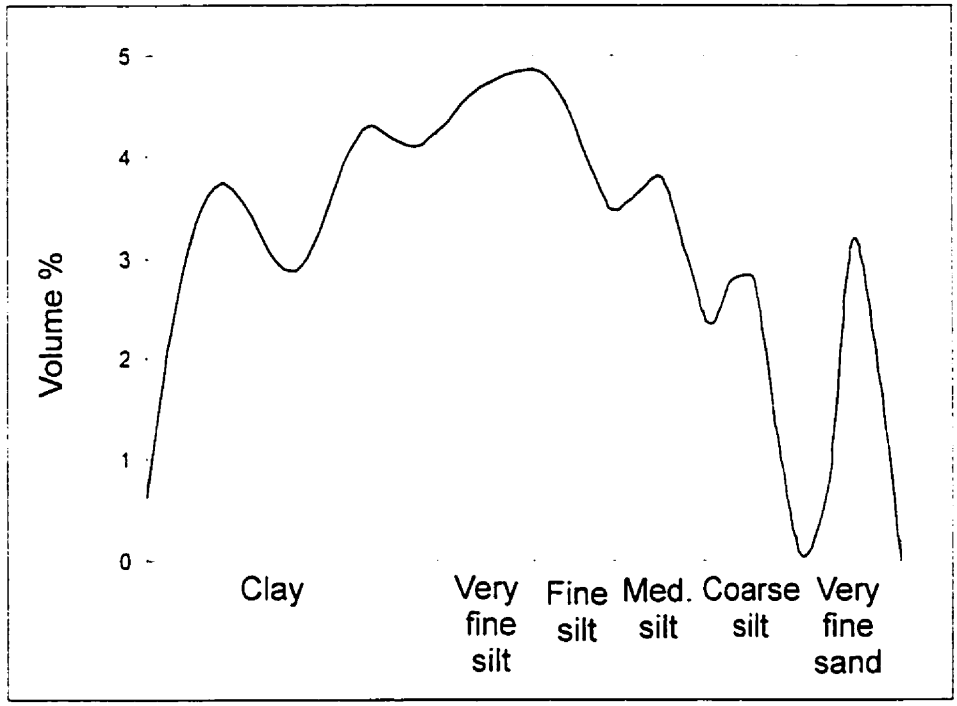

Example of the grain size distribution in a sample from trap B3.